Running title: Senescence manipulation enhances tomato yield

Corresponding author: Magdalena Rossi. Botany Department, Biosciences Institute, University of São Paulo (USP), São Paulo, Brazil.

Article title: Manipulation of a senescence-associated gene improves fleshy fruit yield

Bruno S. Lira [a]; Giovanna Gramegna[a]; Bruna A. Trench[a]; Frederico R.R. Alves[a]; Eder M. Silva[b]; Geraldo F.F. Silva[b]; Venkatesh P. Thirumalaikumar[c]; Alessandra C.D. Lupi[a]; Diego Demarco[a]; Eduardo Purgatto[d]; Fabio T.S. Nogueira[b]; Salma Balazadeh S[c]; Luciano Freschi[a]; Magdalena Rossi[a]

[a] Departamento de Botânica, Instituto de Biociências, Universidade de São Paulo, Rua do Matão, 277, 05508-090, São Paulo, Brasil.

[b] Departamento de Ciências Biológicas, Escola Superior de Agricultura 'Luiz de Queiroz', Universidade de São Paulo, Avenida Pádua Dias, 11, 13418-900, Piracicaba, Brasil.

[c] Plant Signaling Group, Max Planck Institute of Molecular Plant Physiology, 14476 Potsdam-Golm, Germany.

[d] Departamento de Alimentos e Nutrição Experimental, Faculdade de Ciências Farmacêuticas, Universidade de São Paulo, Avenida Prof. Lineu Prestes, 580, 05508-000, São Paulo, Brasil.

One sentence summary: Senescence-associated gene knockdown increases carbon exportation towards sink organs increasing plant yield in Solanum lycopersicum.

List of author contributions:

B.S.L. designed and performed most of the experiments, analysed the data and wrote the article with contributions of all the authors; G.G. designed and performed the confocal and protein-protein interaction experiments and wrote the article with contributions of all the authors; B.T. performed some experiments; F.R.R.A. performed the gas exchange and chlorophyll fluorescence analysis; A.C.D.L. performed some experiments; D.D assisted the preparation of TEM samples and obtained the micrographs; E.P. performed soluble sugar quantification; E.M.S. and G.F.F.S. produced the transgenic plants *OEmiR164a*; F.T.S.N. supervised E.M.S. and G.F.F.S.; V.P.T. generated the transgenic *Atore1* lines overexpressing each *SlORE1* putative ortholog under the supervision of S.B.; L.F. designed the experiments, contributed to data analysis and complemented the writing; M.R. designed the experiments, contributed to data analysis and wrote the article with contributions of all the authors.

Funding information:

B.S.L., G.G., F.R.R.A. and B.T. were recipients of FAPESP fellowships, M.R., F.T.S.N. and D.D. were funded by a fellowship from CNPq. A.C.D.L. was recipient of CAPES fellowship. This work was partially supported by grants from FAPESP (Brazil; 2016/01128-9, 2014/10651-1), CNPq (Brazil), CAPES (Brazil) and USP (Brazil).

Corresponding author e-mail: mmrossi@usp.br

Abstract

Senescence is the process that marks the end of leaves lifespan. As it progresses, the massive macromolecular catabolism dismantles the chloroplasts and, consequently, decreases the photosynthetic capacity of these organs. Thus, senescence manipulation is a strategy to improve plant yield by extending the leaf photosynthetically active window of time. However, it remains to be addressed if this approach can improve fleshy fruit production and nutritional quality. One way to delay senescence initiation is by regulating key transcription factors (TFs) involved in triggering this process, such as the NAC TF ORESARA1 (ORE1). Here, three senescence-related NAC TFs from *Solanum lycopersicum* were identified, namely SlORE1S02, SlORE1S03 and SlORE1S06. All three genes showed to be responsive to senescence-inducing stimuli and post-transcriptionally regulated by the microRNA *miR164*. Moreover, the encoded proteins physically interacted with the chloroplast maintenance related TF SlGLKs. This characterization led to the selection of a putative tomato *ORE1* as target gene for RNAi knockdown. Transgenic lines showed delayed senescence and enhanced carbon assimilation that, ultimately, increased the number of fruits and their total soluble solid content. Additionally, the fruit nutraceutical composition was enhanced. In conclusion, the data provide robust evidence that the manipulation of leaf senescence is an effective strategy for yield improvement in fleshy fruit-bearing species.

Keywords: *Solanum lycopersicum,* tomato, *ORESARA1, GOLDEN2-LIKE,* senescence, yield.

Introduction

The ever-growing demand for food and biofuels has been a significant driving force behind studies focussed on crop yield manipulation. As a complex trait, many strategies can lead to yield improvement, such as manipulation of morphogenetic patterns, source activity, source to sink communication or sink activity (Rossi et al., 2015). Delaying senescence to extend leaf photosynthetic activity is considered one mechanism to strengthen source activity aiming to increase the net carbon availability for sink organs (Thomas & Ougham, 2014; Rossi et al., 2015). The expression of *ISOPENTENYL TRANSFERASE* (*IPT*), which encodes the enzyme responsible for the rate-limiting step in cytokinin biosynthesis, under the control of the *SENESCENCE ASSOCIATED GENE 12* (*SAG12*) promoter has been extensively used for delaying leaf senescence (Gregersen et al., 2013). Once the expression is activated during senescence by the *SAG12* promoter, the increment in cytokinin levels blocks senescence progression thereby retaining photosynthetically active leaves. This approach has proven to successfully block or attenuate both age- and stress-related leaf senescence in different crop species like rice (Liu et al., 2010), cassava (Zhang et al., 2010), wheat (Sykorova et al., 2008) and tomato (Swartzberg et al., 2006).

With the increase in the knowledge about the genetic control of senescence, transcription factors (TFs), such as those belonging to the WRKY, MYB and NAM/ATAF1/CUC2 (NAC) families, stand out as regulators of this process (Balzadeh et al., 2008). The extensive NAC family regulates a diversity of processes along plant development (Mitsuda et al., 2005, Olsen et al., 2005, Puranik et al., 2012). Particularly, the *Arabidopsis thaliana ORESARA1* gene (*AtORE1)* has received special attention for encoding a master regulator of senescence initiation (Oh et al., 1997, He et al., 2005, Kim et al., 2009, Balazadeh et al., 2010, Kim et al., 2011, Rauf et al., 2013), as *Atore1* mutant exhibits a delayed senescence phenotype (Oh et al., 1997, Kim et al., 2009). Besides being induced by ethylene, salt, darkness and abscisic acid (Kim

et al., 2009, Balazadeh et al., 2010, Kim et al., 2011, Sakuraba et al, 2014; Song et al., 2014,) *AtORE1* is also post-transcriptionally regulated by microRNA *miR164* (Kim et al., 2009). AtORE1 not only induces senescence-related genes, but also physically interacts with and inactivates the chloroplast maintenance-related TF GOLDEN2-LIKE (GLK), shifting the cell from a photosynthetically active program towards senescence (Rauf et al., 2013, Garapati et al., 2015). GLKs have been shown to control chloroplast development in several species, in which usually a pair of paralogs with functional redundancy occurs in the genome of several species (Fitter et al., 2002, Waters et al., 2008, 2009). In tomato, *Solanum lycopersicum*, the paralogs exhibit organ specificity; while *SlGLK1* is mostly expressed in vegetative organs, *SlGLK2* is exclusively transcribed in the stylar portion of the fruits (Powell et al, 2012, Nguyen et al., 2014). Interestingly, *Slglk2* mutation, which was fixed in many cultivated varieties, negatively impacts fruit chloroplast differentiation; on the other hand, *SlGLK2* overexpression increases fruit starch, soluble sugar and carotenoid content (Powell et al., 2012).

Although being a model plant for fleshy fruit physiology, the senescence regulatory network and its impacts on fruit development and quality in tomato remains elusive. Here, putative *AtORE1* orthologs, namely *SlORE1S02, SlORE1S03* and *SlORE1S06,* were identified in tomato genome. The genes were functionally characterised regarding their responsiveness to senescence-inducing treatments, regulation by *SlmiR164* and capability to physically interact with SlGLKs and to complement *Atore1* mutant phenotype. Moreover, *SlORE1S02*-knockdown plants displayed delayed senescence, enhanced carbon assimilation and altered source-sink sugar partitioning leading to the development of more fruits with increased soluble sugar content. The results obtained provide robust evidences that the manipulation of leaf senescence is a promising strategy for yield improvement in the fleshy fruit-bearing species.

Results

Solanum lycopersicum genome harbours three putative senescence-related *AtORE1* orthologs

To identify putative *S. lycopersicum AtORE1* orthologs, the protein sequences of all NAC transcriptions factors of *S. lycopersicum* and *A. thaliana,* retrieved from the Plant Transcription Factors Database (http://planttfdb.cbi.pku.edu.cn/), were aligned (Supplemental Table 1). The phylogenetic reconstruction (Supplemental Fig. S1) allowed the selection of three putative NAC domain-containing proteins (Supplemental Fig. S2), named SlORE1S02, SlORE1S03 and SlORE1S06 accordingly to the chromosome localization (Fig. 1). Then, their responsiveness to senescence-inducing treatments was addressed.

The transcript profile of *SlORE1S02*, *SlORE1S03* and *SlORE1S06* was evaluated upon different *in vitro* treatments for senescence induction, *i.e.* treatment with ethylene, darkness, jasmonic acid, salicylic acid or salt (Fig. 2). Confirming the induction and progression of senescence, all treatments triggered significant reduction in leaf chlorophyll content as well as down- and up-regulation of *SlGLK1* (the chloroplast maintenance-related TF) and *SlSAG12* (the senescence-associated gene) genes, respectively (Supplemental Fig. S3). The mRNA profile of the three *SlORE1*s was modulated by the various treatments. While *SlORE1S03* was induced in all cases, the level of *SlORE1S02* mRNA increased upon the application of ethylene, salicylic acid and salt solution, and *SlORE1S06* was upregulated by ethylene and darkness. Thus, although with differences, all three genes were transcriptionally activated by senescence-inducing stimuli.

The transcriptional profile of *SlORE1*s during fruit development and ripening was also assessed (Fig. 3). For all three *SlORE1*s, the highest expression levels were identified at early immature stages declining towards the ripe stage. Thus, although in leaves these genes were induced by ethylene, mRNA accumulation did not coincide with the ripening-associated climacteric peak of ethylene production typically observed at the breaker (BR) stage. This result indicates that,

Figure 1

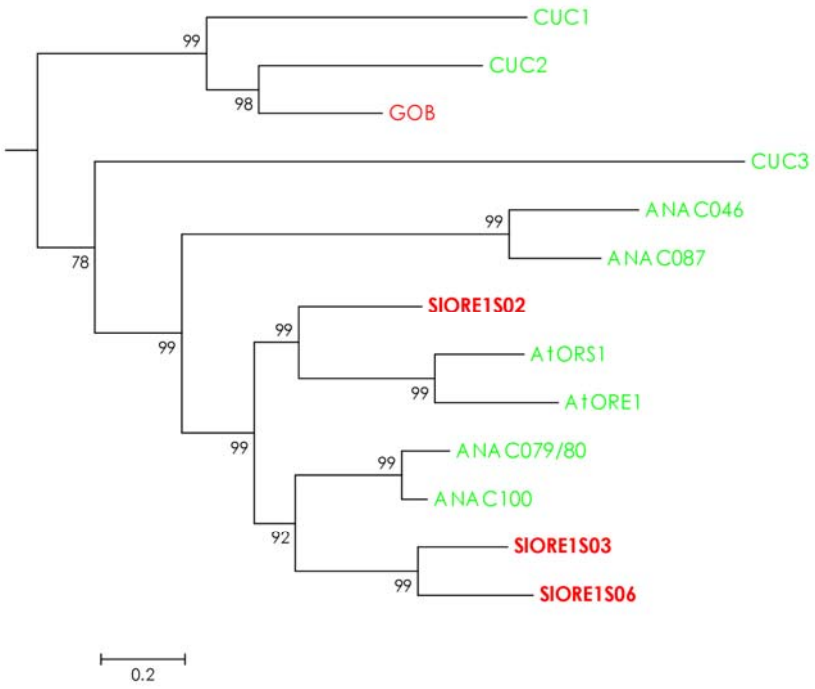

Figure 1. Phylogenetic representation of the NAC transcription factor subfamily that includes AtORE1 and SlORE1s. Detail of the phylogenetic reconstruction obtained from the alignment of the protein sequence of all NAC transcription factors of *Arabidopsis thaliana* (green) and *Solanum lycopersicum* (red) obtained from the Plant Transcription Factor Database (Supplemental Table 1). Three putative AtORE1 orthologs (in bold), named SlORE1S02, SlORE1S03 and SlORE1S06 according to their chromosome position, were identified.

although a role in early fruit development cannot be ruled out, a direct function of *SlORE1*s along fruit ripening seems unlikely, as revealed by the expression pattern in this organ. Moreover, the data suggest an organ-specific ethylene-mediated regulation of *SlORE1* genes.

Figure 2

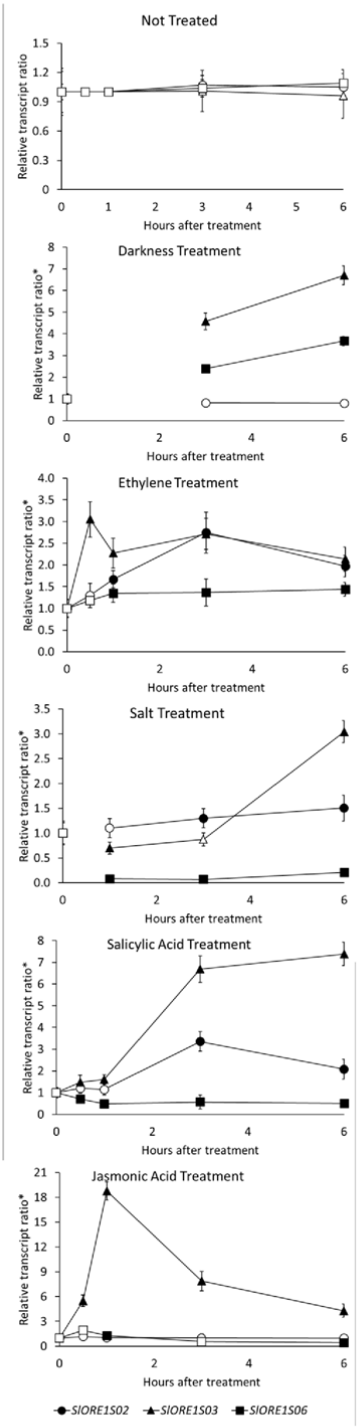

Figure 2. Transcript profile of *SlORE1s* in response to senescence-inducing treatments. Transcript profile of *SlORE1*s in leaves of 4-week-old *in vitro*-grown plants after senescence-inducing treatments. Values represent the mean ± SE from at least three biological replicates normalized against the zero hour sample. Each treatment relative transcript ratio is expressed as the ratio between treatment value and the corresponding untreated control (*). Statistically significant differences relative to the zero hour treatment are represented with closed symbols ($P < 0.05$).

***SlORE1*s are regulated by *SlmiR164* and their encoded proteins physically interact with SlGLKs and partially recover the *Atore1* phenotype**

Figure 3

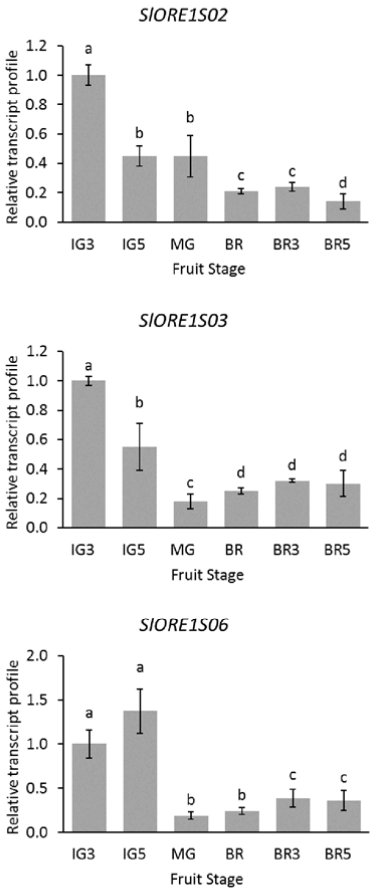

Figure 3. Transcript profile of *SlORE1s* along fruit development and ripening. IG: immature green stage; MG: mature green stage; BR: breaker stage; BRX: X days after breaker stage. Values represent the mean ± SE from at least three biological replicates normalized to the corresponding IG3 sample. Statistically significant differences are represented with letters ($P < 0.05$).

151 *In silico* analysis of the coding sequences revealed putative binding sites for *SlmiR164* in all
152 three *SlORE1s*. However, this site is disrupted by an insertion of 29 bp in *SlORE1S02* (Fig. 4A).
153 To ascertain if this insertion affects *SlmiR164* recognition, a modified 5' RACE was performed

Figure 4

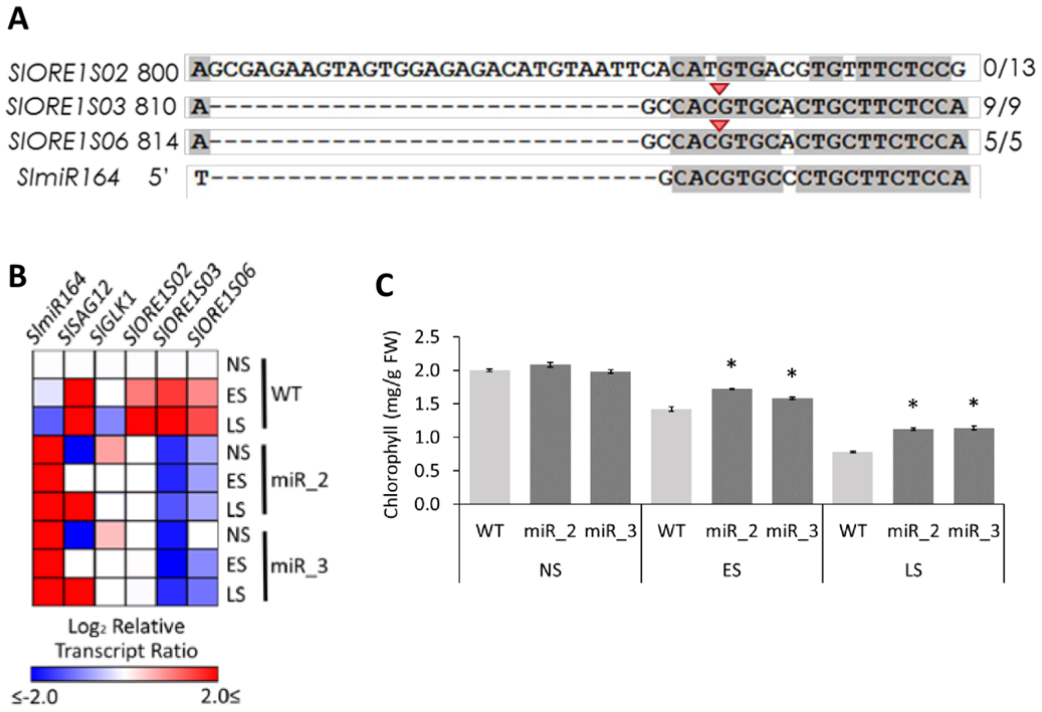

Figure 4. Regulation of *SlORE1*s by *SlmiR164*. **A**, Highlight of the alignment of *SlORE1*s and *SlmiR164* showing the putative binding site. The validation by a modified 5' RACE assay identified cleaved transcripts of *SlORE1S03* and *SlORE1S06*. The red arrowhead and numbers on the right indicate the inferred cleavage site and the fraction of positive cloned PCR products ending at the site, respectively. Shading threshold of alignment = 75%. **B**, Heatmap representing the transcript profile of non-senescent (NS), early senescing (ES) and late senescing (LS) leaves of wild type control (WT) and *OEmiR164a* (lines miR_2 and miR_3) genotype. Values represent mean of at least three biological replicates normalised against the NS WT sample. Statistically significant differences in comparison to NS WT are represented as coloured squares ($P < 0.05$). The relative transcript values are detailed in Supplemental Table S2. **C**, Chlorophyll content in NS, ES and LS leaves. Values represent the mean ± SE from at least three biological replicates. Asterisks denote statistically significant differences to WT control ($P < 0.05$.)

154 to detect cleaved transcripts, using RNA extracted from non-senescing leaves. This allowed the
155 identification of *SlmiR164*-guided cleavage transcripts of *SlORE1S03* and *SlORE1S06*, but not of
156 *SlORE1S02* (Fig. 4A).

To gain further knowledge about the role of *SlmiR164* for *SlORE1*s regulation, the mRNA of the three genes was profiled in transgenic lines harbouring a 35S:*AtMIR164a* construct (abbreviated as *OEmiR164a*) in non-senescent, early senescing and late senescing leaves (Fig. 4B). The mRNA pattern of *SlGLK1* and *SlSAG12* was also assessed as senescence markers. In wild-type plants (WT), leaf senescence was accompanied by a progressive downregulation in *SlmiR164* and *SlGLK1* and upregulation of *SlSAG12, SlORE1S02, SlORE1S03* and *SlORE1S06.* As expected, *OEmiR164a* lines displayed high levels of *SlmiR164* in both, non-senescent and senescent leaves stages. As a result, a lag in *SlGLK1* decrease and *SlSAG12* accumulation, together with the increased chlorophyll levels, were indicatives of delayed senescence initiation (Fig. 4C). The marked reduction of *SlORE1S03* and *SlORE1S06* mRNA levels observed in *OEmiR164a* lines is in agreement to both being directly regulated by *SlmiR164*. Interestingly, the levels of *SlORE1S02* in non-senescent and senescing leaves were the same as those observed in non-senescent WT leaves, meaning that the maintenance of high levels of *SlmiR164* prevented the senescence-associated induction of this gene. Although *SlmiR164* is not capable of cleaving *SlORE1S02* transcripts, it regulates it by targeting a currently unknown factor that, in turn, drives the senescence-associated mRNA accumulation of this gene. Thus, *SlmiR164* directly controls the transcript levels of *SlORE1S03* and *SlORE1S06* and indirectly regulates the transcript abundance of *SlORE1S02*, what is in line with the known transcriptional regulation of *AtORE1* by *AtmiR164* (Kim et al., 2009).

Moreover, AtORE1 is known to physically interacts with AtGLKs in the nucleus, preventing the activity of these chloroplasts maintenance TFs (Rauf *et al.,* 2013*)*. Then, it was first addressed whether SlORE1s and SlGLKs are nucleus-targeted proteins. Confocal analysis of *Nicotiana tabacum* leaves transiently expressing transcription factor - GFP fusion proteins revealed that SlORE1S02, SlORE1S03, SlORE1S06, SlGLK1 and SlGLK2 were localized in the nucleus as the GFP fluorescence in all cases co-localized with the fluorescence of the DAPI marker (Supplemental Fig. S4). For the latter, the result confirmed that previously reported in tomato protoplasts by

Figure 5

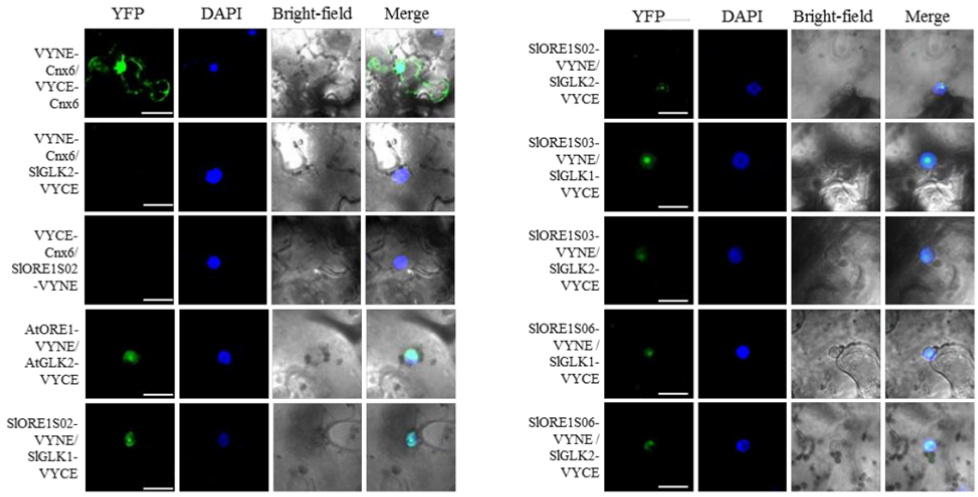

Figure 5. Analysis of SlGLKs and SlORE1s protein-protein interaction by Bimolecular Fluorescent Complementation (BiFC). VYNE and VYCE fusion proteins were transiently expressed in *N. tabacum* leaves by infiltration with *A. tumefaciens.* VYNE-Cnx6/VYCE-Cnx6 and AtORE1/AtGLK2 (Gehl et al., 2009) were used as technical and biological positive controls, respectively. VYNE-Cnx6/SlGLK2-VYCE and VYCE-Cnx6/SlORE1S02-VYNE interactions were used as negative controls. SlOREs/SlGLKs interaction was confirmed as evidenced by the YFP fluorescence detected. YFP, DAPI nuclear marker, bright-field and merged signals are indicated above the panels. Bars = 20 µm, except in VYNE-Cnx6/VYCE-Cnx6 images = 40 µm.

183 Tang et al. (2015). Next, bimolecular fluorescence complementation (BiFC) was used to test
184 the physical interaction. The C-terminal of SlORE1s and SlGLKs were fused to the N- (VYNE) and
185 C- terminal (VYCE) of the Venus YPF protein, respectively (Fig. 5). The interaction between

AtORE1 and AtGLK2 was used as positive control. In all interactions tested, fluorescence was detected in the nucleus, thus, all SlORE1s physically interact with both SlGLKs. Of note, a strong fluorescence signal was observed in the nucleolus in all SlORE1-SlGLK interactions, and also for AtORE1 and AtGLK2.

It has been suggested that the ubiquitin proteasome system may be active in the nucleolus, where ubiquitin and proteasome were immunolocalized (Stępiński, 2012). In addition, this compartment provides a site for transient inactivation of enzymatic or regulatory proteins (Stępiński, 2014). As SlGLK2 was shown to be degraded by the ubiquitin-proteasome system (Tang et al., 2015), one may speculate that the ORE1-GLK complex is transferred to the nucleolus where GLKs are inactivated by ubiquitination and subsequently degraded in this compartment.

These results show similarities between *SlORE1*s and *AtORE1* regulation. To address whether *SlORE1s* were able to recover the *Atore1* delayed-senescence phenotype, each *SlORE1*s was constitutively overexpressed in the Arabidopsis mutant background, *Atore1*-OE:*SlORE1S02*, *Atore1*-OE:*SlORE1S03* and *Atore1*-OE:*SlORE1S06*. In line with *AtORE1* overexpression in Col-0 background (Rauf et al., 2013), no visible phenotype was observed in young plants. Dark-induced senescence was assayed in detached leaves. After seven days, while *Atore1* leaves remained green, the leaves overexpressing any of the *SlORE1*s acquired a yellowish tone indicative of ongoing senescence, but not to the same extent as the Col-0 genotype (Fig. 6). Thus, all three *SlORE1*s were able to partially recover the senescence delay in *Atore1* mutant.

SlORE1S02-knockdown in tomato increases photosynthesis and delays dark-induced senescence

Among the three *SlORE1*s, *SlORE1S02* was chosen for stable RNA interference (RNAi) knockdown as this is the closest ortholog to *AtORE1* in the phylogenetic reconstruction, its transcript levels are highly modulated along senescence and indirectly regulated by *SlmiR164*,

Figure 6

Figure 6. *SlORE1s* partially recover *Atore1* senescence impairment. Detached leaves from three-month-old Col-0, *Atore1* mutant, *Atore1-OE:SlORE1S02*, *Atore1-OE:SlORE1S03* and *Atore1-OE:SlORE1S06* plants were kept in darkness for seven days to induce senescence. While *Atore1* displayed no signs of senescence, the yellowish colour of the genotypes overexpressing *SlORE1s* hints an ongoing senescence program, yet not to the extent observed in the Col-0 genotype. Bar = 1 cm.

212 and the encoded protein physically interacts with SlGLKs and partially complement the *Atore1*
213 mutant. Five tomato transgenic lines were obtained and three lines displaying over 70%
214 silencing (Supplemental Fig. S5), namely L1, L3 and L6, were chosen for further phenotyping.

Interestingly, *SlORE1S03* and *SlORE1S06* were also reduced in leaves of *SlORE1S02*-knockdown lines, but not to the same extent as *SlORE1S02.* Since there is an extremely low degree of similarity among the RNAi target region of *SlORE1S02* and the coding sequences of *SlORE1S03* and *SlORE1S06,* the possibility of cross-silencing can be ruled-out. Instead, it is likely that *SlORE1S02* is an upstream positive regulator of *SlORE1S03* and *SlORE1S06* (Supplemental Fig. S6).

Gas exchange and chlorophyll fluorescence parameters were measured by using an infra-red gas analyser (IRGA) at two developing stages of the plant: (I) before the beginning of flowering stage, in the fifth leaf of 70-day-old plants (referred as young plant leaves - YPL), and (II) in fruit-bearing stage, in the sixth leaf of 120-day-old plants (referred as mature plant leaves - MPL). No differences were found in photosynthetic parameters in YPL. However, MPL from *SlORE1S02*-knockdown plants showed increased carbon assimilation (*A*) in comparison to the untransformed control genotype (MT), while all other measured parameters remained unaltered (Table 1).

Chlorophyll levels in YPL and MPL were higher in transgenic plants than in equivalent leaves of the MT genotype (Fig. 7A). Whereas, at MPL stage, the density of chloroplasts per mesophyll cell was slightly higher in transgenic lines (Fig. 7B), the ultrastructure of this organelle was not affected by the downregulation of *SlORE1S02* (Supplemental Fig. S7). Accordingly, *SlGLK1* mRNA levels were higher in both YPL and MPL of transgenic plants (Fig. 7C). Interestingly, while the senescence marker *SlSAG12* was undetectable in YPL, lower levels were detected in transgenic MPL compared to the corresponding MT control (Fig. 7C). Together these results suggest a delay in senescence in *SlORE1S02*-knockdown plants. To further corroborate this hypothesis, the eighth leaf of 120-day-old plants was detached and kept in the dark for 10 days. While MT leaves turned yellowish, transgenic ones kept greenness, supporting the conclusion that *SlORE1S02* deficiency delays senescence (Fig. 7D).

Figure 7

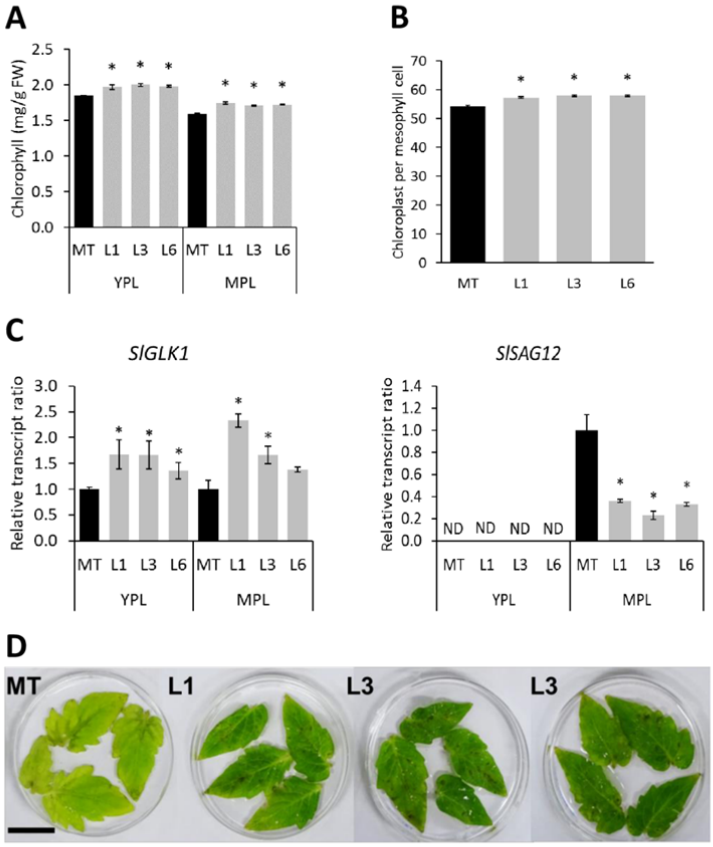

Figure 7. *SlORE1S02-knockdown* affects leaf aging. **A**, Chlorophyll content in leaves. Values represent the mean ± SE from at least three biological replicates. Asterisks denote statistically significant differences to MT control ($P < 0.05$). YPL: young plant leaves; MPL: mature plant leaves. **B**, Number of chloroplasts per mesophyll cell of MPL. Values represent the mean ± SE from at least 45 cells. Asterisks denote statistically significant differences to MT control ($P < 0.05$). **C**, *SlGLK1* and *SlSAG12* transcript ratio in YPL and MPL leaves. Values represent the mean ± SE from at least three biological replicates normalised against the respective sample from MT control. Asterisks denote statistically significant differences to MT control ($P < 0.05$). The relative transcript values are available in Supplemental Table S4. **D,** *SlORE1S02*-knockdown effect on dark-induced senescence in tomato leaves. Detached leaflets from 120-day-old plants kept ten days in darkness retain greenness, while MT control leaflets turned yellow. Bar = 5 cm.

***SlORE1S02-knockdown* in tomato increases yield and brix**

As transgenic plants assimilate carbon for an extended period of time, the impact of *SlORE1S02-knockdown* over yield was evaluated. Transgenic plants produced more fruits than

Figure 8

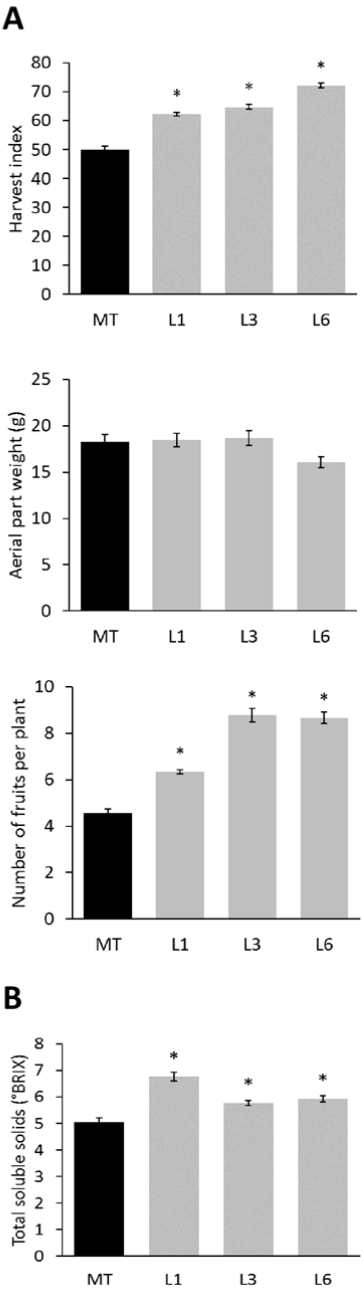

Figure 8. *SlORE1S02*-knockdown increases yield and *brix*. **A**, Harvest index, aerial part weight and ripe fruit number in MT and *SlORE1S02*-knockdown lines. Values represent the mean ± SE from at least six biological replicates. Asterisks denote statistically significant differences compared to MT control genotype ($P < 0.05$). **B**, Total soluble solids of ripe fruits measured in *brix* units. Values represent the mean ± SE from at least twelve biological replicates. Asterisks denote statistically significant differences compared to MT control genotype ($P < 0.05$).

244 MT control plants, rendering a significant increase in harvest index (HI), as no difference was
245 detected in aerial shoot mass (Fig. 8A). The transgenic fruits showed no alteration in the shape,
246 weight and diameter (Supplemental Fig. S8). Besides, *SlORE1S02*-knockdown lines showed

247 higher levels of soluble solids in ripe fruits as reflected by the increment in *brix* units (Fig. 8B),
248 which is also an important trait in tomato, especially for industrial processing.
249 Enhanced HI and *brix* are typically due to increased levels of glucose, fructose and sucrose and
250 are indicative of altered carbohydrate metabolism. Thus, the content of starch and soluble
251 sugars in leaves and fruits was determined (Fig. 9). The fruits of transgenic plants showed an
252 increased content of glucose in all analysed stages and of fructose in both ripening stages,
253 which explains the increment in *brix* units. Moreover, starch content in mature green and
254 breaker fruits of *SlORE1S02*-knockdown lines were also higher when compared to MT control.
255 As expected, six days after the breaker stage, starch was totally degraded in all genotypes. In
256 leaves, while YPL of transgenic plants accumulated higher starch and sucrose levels than MT
257 control genotype; when fruits are developing, in the MPL, the allocation of fixed carbon as
258 starch diminished, whereas sucrose still accumulated at higher levels. The upregulation in the
259 leaf carbohydrate levels triggered by *SlORE1S02*-knockdown is consistent with the above-
260 mentioned increase in carbon assimilation observed in the transgenic lines. Moreover,
261 considering that in tomato carbon is mostly translocated as sucrose (Barker et al., 2000), this
262 carbohydrate pattern suggests an enhanced carbon export from leaves towards sink organs in
263 SlORE102-deficient plants.
264
265 **Isoprenoid metabolism is affected by *SlORE1S02*-knockdown tomato plants**

266 It was shown that lowering *SlORE102* transcript abundance affects chlorophyll accumulation
267 and carbon assimilation and partitioning. To better understand the origin of these metabolic
268 alterations and their impact of fruit chemical composition, isoprenoid-derived compounds (*i.e.*
269 chlorophyll, tocopherols and carotenoids, Supplemental Table S3) were quantified and the
270 mRNA levels of chlorophyll-, tocopherol- and carotenoid-metabolism associated genes profiled
271 (Supplemental Table S4) (Fig. 10). The analysed genes were those that showed to be
272 transcriptionally regulated key points of the biosynthetic pathways (Quadrana et al., 2013;

Figure 9

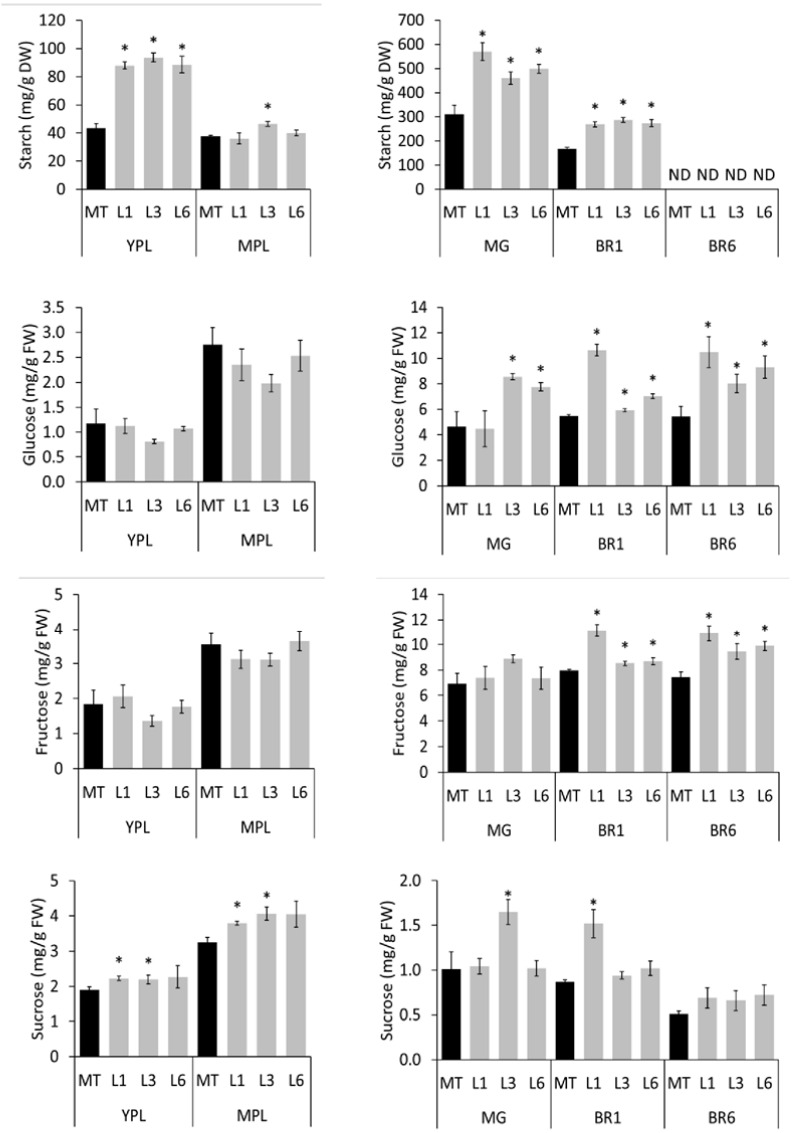

Figure 9. *SlORE1S02*-knockdown alters sugar profile in leaves and fruits. Content of starch and soluble sugars in leaves and fruits of *SlORE1S02*-knockdown lines. Values represent the mean ± SE from at least three biological replicates. Asterisks denote statistically significant differences to MT control genotype ($P < 0.05$). ND: Not detected. YPL, young plant leaves; MPL, mature plant leaves; MG, mature green stage; BR, breaker; BR6: 6 days after BR, respectively.

273 Almeida et al., 2015, 2016). The transcript abundance of those paralogs that, based on
274 previous reports, were not directly involved in the analysed pathways in the sampled organs
275 was not addressed. This is the case of *SlPPHL2* and *SlPPHL3,* which are extremely low

Figure 10

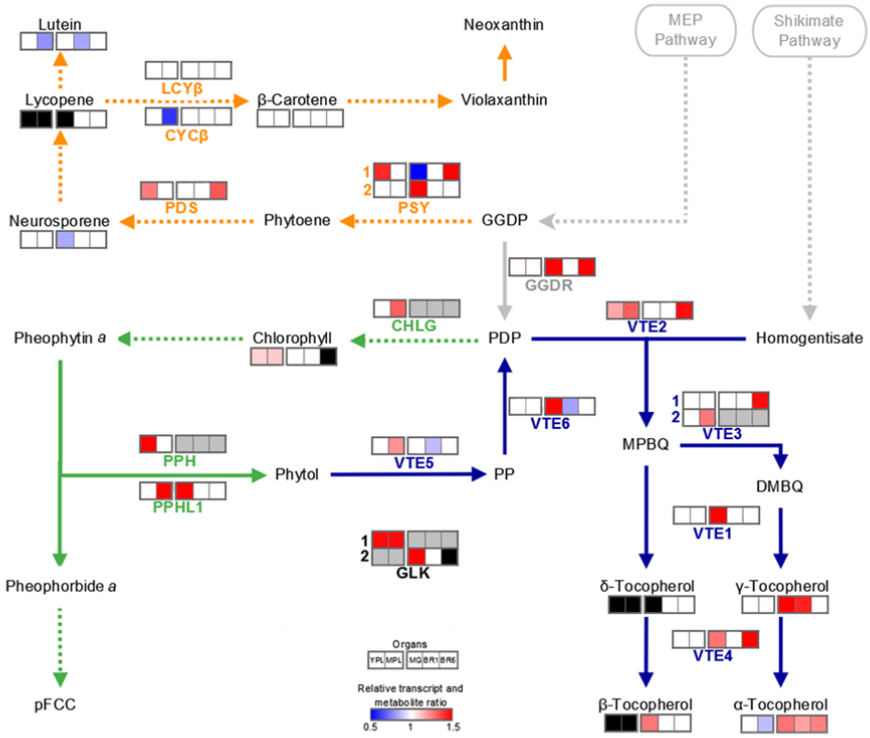

Figure 10. Isoprenoid metabolism. Schematic representation of the interconnection between Chl synthesis and degradation (green), carotenogenesis (orange) and tocopherol biosynthetic (blue) pathways. Dotted lines denote that intermediate steps were omitted. The heatmap represents statistically significant differences in relative transcript and metabolite amounts detected in *SlORE1S02*-knockdown lines compared to the corresponding organ of MT control genotype ($P < 0.05$). For simplicity, the mean of the three transgenic line values is represented when, at least, two were statistically significant different than MT control. The absolute metabolite and relative transcript values are detailed in Supplemental Table S3 and S4. Black and grey colours indicate that transcripts were not detected or not addressed, respectively. Enzymes and compounds are named according to the following abbreviations: GGDR, geranylgeranyl diphosphate reductase; PSY, phytoene synthase; PDS, phytoene desaturase; LCYβ, chloroplast-specific β-lycopene cyclase; CYCβ, chromoplast-specific β-lycopene cyclase; GGDP, geranylgeranyl diphosphate; PDP, phytyl diphosphate; PP, phytyl phosphate; CHLG, chlorophyll synthase; PPH, pheophytinase; PPHL1, pheophytinase-like 1; pFCC, primary fluorescent chlorophyll catabolite; VTE5, phytol kinase; VTE6, phytyl phosphate kinase; MPBQ, 2-methyl-6-geranylgeranylbenzoquinol; VTE1, tocopherol cyclase; VTE2, homogentisate phytyl transferase; VTE3, 2,3-dimethyl-5-phytylquinol methyltransferase; VTE4, tocopherol C-methyl transferase; MEP, methylerythritol 4-phosphate. Adapted from Almeida et al. (2016).

276 expressed (Lira et al., 2015) and, differently from *SlPPHL1*, are not functionally characterised
277 (Lin et al., 2016); *SlPSY3* is involved in root carotenogenesis (Liu et al., 2015); and *SlLCYβ2*
278 (Solyc10g079480) and *SlGGDR1* (Solyc01g088310) are poorly expressed in the analysed organs

279 (transcriptional data available on TomExpress database -
280 http://gbf.toulouse.inra.fr/tomexpress/).

281 In MPL of *SlORE1S02*-knockdown plants, the chlorophyll recycling/biosynthesis was enhanced,
282 as evidenced by the increase in *CHLOROPHYLL SYNTHASE* (*SlCHLG*), *PHEOPHYTINASE-LIKE 1*
283 (*SlPPHL1*) and *PHYTOL KINASE* (*SlVTE5*) transcript abundance. Although the mRNA levels of
284 *PHYTOENE SYNTHASE 1* (*SlPSY1*) and *PHYTOENE DESATURASE* (*SlPDS*) were increased in YPL, no
285 differences were found in leaf carotenoid contents, except for a slight reduction in lutein from
286 MPL. Regarding tocopherol synthesis, YPL showed similar levels of tocopherol in both
287 genotypes, which is in line with the expression of the enzyme encoding genes that supply
288 phytyl diphosphate (PDP) precursor, such as *GERANYLGERANYL DIPHOSPHATE REDUCTASE*
289 (*SlGGDR)*, *SlVTE5* and *PHYTYL PHOSPHATE KINASE* (*SlVTE6*). However, in *SlORE1S02*-
290 knockdown MPL, due to chlorophyll biosynthesis enhancement, PDP availability for tocopherol
291 synthesis is reduced compared to MT control resulting in reduced levels of this compound. It is
292 worth mentioning that the most abundant form of vitamin E is α-tocopherol that perfectly
293 correlates with the amount of total-tocopherol (Supplemental Table S3). Apparently, the
294 maintenance of a highly active photosynthetic apparatus in MPL requires less amounts of
295 antioxidant tocopherol compounds.
296 The impact of *SlORE102*-knockdown on fruit isoprenoid profile was distinct from those
297 observed in leaves. There was no difference in fruit chlorophyll content between transgenic
298 and control plants. Similarly, carotenoid metabolism remained almost unaffected, displaying
299 punctual reductions in neurosporene and lutein content in MG and BR1 fruits, respectively.
300 Tocopherols were more abundant in *SlORE1S02*-knockdown than in control fruits, which is in
301 accordance to the transcript levels of *SlGGDR*, *SlVTE6*, *HOMOGENTISATE PHYTYL TRANSFERASE*
302 (*SlVTE2)*, *2,3-DIMETHYL-5-PHYTYLQUINOL METHYLTRANSFERASE* (*SlVTE3(1))*, *TOCOPHEROL*
303 *CYCLASE* (*SlVTE1)* and *TOCOPHEROL C-METHYL TRANSFERASE* (*SlVTE4)*.

304 Therefore, *SlORE1S02*-knockdown plants showed organ-specific regulation of isoprenoid
305 metabolism.
306
307

Discussion

The leaves are the major photosynthetic organs and the net carbon fixed during the photosynthetic period is critical for plants' fitness and sink organ development (Wu et al, 2012). Thus, source-sink relationship is tightly linked to leaf lifespan and, consequently, affected by the fine control of senescence. In this regard, a straightforward approach to increase yield is to extend the photosynthetic function phase. This has been achieved in grasses by silencing NAC TF encoding genes. Although an increase in grain yield was observed due to extended grain filling time, seed quality was compromised by reduced nutrient remobilization (Waters et al., 2009; Liang et al., 2014). Yet, the impact of delayed senescence remains poorly explored in non-monocarpic species that do not undergo whole-plant senescence after the reproductive phase (Thomas, 2012).

To gain insight on how fleshy fruit development and yield can be affected by altering leaf senescence, the senescence master regulator *ORE1* was targeted in *S. lycopersicum*. Three putative orthologs were identified in the tomato genome, namely *SlORE1S02*, *SlORE1S03* and *SlORE1S06*. As all were induced by senescence-inducing treatments, regulated by *SlmiR164,* able to physically interact with SlGLKs and capable to rescue *Atore1* mutant*, SlORE1S02*, the phylogenetically closest one to *AtORE1*, was chosen for knockdown by RNA interference.

The reduction in the amount of *SlORE1S02* transcripts affected the metabolism of source leaves, both of young and mature plants. The increase in chlorophyll content and the expression of *SlGLK1* TF, together with the increment in carbon assimilation and the reduced *SlSAG12* mRNA levels in leaves of mature plants, hint that senescence is delayed in transgenic plants. This was corroborated by the dark induction senescence assay on detached leaves. The aforementioned phenotype in leaves from the *SlORE1S02*-deficient plants might be explained, at least in part, because GLK TFs are known to coordinate the expression of genes related to chlorophyll synthesis (*e.g. PROTOCHLOROPHYLLIDE OXIDOREDUCTASE*) and the photosynthetic

machinery (*e.g.* light harvesting complex proteins) leading to proper chloroplast differentiation and maintenance (Waters et al., 2009; Nguyen et al., 2014). This is in agreement with the increased chloroplast number in mesophyll cells of mature leaves. Additionally, higher levels of *SlCHLG* transcript, whose encoded protein is a key enzyme for chlorophyll biosynthesis and also regulates the synthesis of chlorophyll-binding proteins (Shalygo et al., 2009), contributes to the extended photosynthetic active period in transgenic plants.

Tocopherol metabolism was also affected in leaves of *SlORE1S02*-knockdown plants. As chlorophyll, tocopherols are isoprenoid-derived compounds that play a main role in protecting photosynthetic machinery by either quenching oxygen singlet ($^1O_2$) or inhibiting the progression of lipid peroxidation (Havaux et al., 2005). It has been demonstrated that the recycling of chlorophyll degradation-derived phytol is the main source of tocopherol side chain in tomato (Almeida et al., 2015). In agreement with this, the delayed senescence progression proposed above for *SlORE1S02*-knockdown plants explains the reduction in tocopherol content measured in leaves from mature plants. In this sense, it has been suggested that increasing tocopherol content along senescence contributes to the proper dismantling and recycling of plastid thylakoid lipids (Chrost et al., 1999). Additionally, the boost in chlorophyll turnover, evidenced by the increment in mRNA abundance of *SlPPHL1* (Lin et al., 2016), *SlVTE5* (Almeida et al., 2016) and *SlCHLG*, driving PDP towards chlorophyll synthesis, further support this statement.

The delayed senescence progression was also reflected in both leaf and fruit sugar composition. During the vegetative phase, before the onset of flower anthesis, while the fifth leaf from control young plants were the main source of assimilates for sink organs, in *SlORE1S02*-deficient plants, these leaves retained higher levels of fixed carbon mainly as starch, as older leaves retained high photosynthetic activity. As fruits began to develop, the starch was remobilised to sucrose and reallocated to these organs. The boosted carbon exportation in *SlORE1S02*-knockdown plants increased yield as the result of the increment in

fruit number. Interestingly, the fruits developed slightly faster than the control genotype as the number of days to reach the breaker stage was reduced (Supplemental Fig. S9A). Additionally, BR1 and BR6, but not MG fruits were enriched in total soluble protein content, which might indicate that *SlORE1S02*-knockdown affect protein degradation during chloroplast-chromoplast transition (Supplemental Fig. S9B).

Regarding fruit nutritional quality, *SlGGDR* mRNA accumulated to higher levels in transgenic fruits during ripening increasing PDP availability for tocopherol synthesis. Moreover, in *SlORE1S02*-knockdown genotype, the tocopherol biosynthesis-related genes were upregulated along fruit ripening, contributing to the increment of this nutraceutical.

Altogether, the metabolic alterations indicate that *SlORE1S02* deficiency delays ageing by means of extending chloroplast maintenance and carbon assimilation. Consequently, photoassimilate exportation towards fruits is enhanced, ultimately, improving harvest index and the content of tocopherol antioxidant and soluble sugars in ripe fruits. Thus, the data obtained suggests that the manipulation of leaf senescence is a promising strategy to improve fleshy fruit yield and metabolism.

Materials and Methods

Plant material, growth conditions and sampling

In vitro treatments for senescence induction were performed with wild type *Solanum lycopersicum* (cv Micro Tom, MT) harboring the wild-type allele *SlGLK2*. Tomato seeds were surface sterilized, sown and cultivated *in vitro* as described by Lira et al. (2014). Four-week-old plants had senescence induced either by application of ethylene (gaseous to a final concentration of 5 $M.L^{-1}$), jasmonic acid (gaseous to a final concentration of 30 µM), salicylic acid (liquid solution to a final concentration of 30 µM), salt (liquid NaCl solution to a final

385 concentration of 300 mM) or kept in darkness. Leaf samples were collected 30 min, 1 h, 3 h, 6
386 h, 48 h-after treatment.
387 For *SlORE1*s fruit transcriptional profiling, tomato plants were grown in 1-L pots in a
388 greenhouse under automatic irrigation in an average mean temperature of 25°C, 11.5/13
389 (winter/summer) light hours and 250-350 µmol m^{-2} s^{-1} of incident photo-irradiance. The
390 pericarp from the top portion of the fruit was sampled at immature green 3 (IG3), immature
391 green 5 (IG5), mature green (MG), breaker (BR), breaker + 3 (BR3) and breaker + 5 (BR5) stages
392 were harvested approximately at 10, 22, 37 (displaying jelly placenta) and, approximately, 42
393 (when the first signals of carotenoid accumulation are visualized), 45 and 48 days after
394 anthesis, respectively. All samples were frozen in liquid N_2, powdered and stored at -80°C.
395 The transgenic lines overexpressing *AtMiR164a* (miR_2 and miR_3) were generated via a 176
396 bp fragment encompassing the *AtMIR164a* precursor (MIR164aAt2g47585) that was amplified
397 from genomic DNA of *Arabidopsis thaliana* ecotype Columbia (Col-0). The PCR product was
398 sub- cloned into TOPO TA (Invitrogen, http://www.lifetechnologies. com) and sequenced. The
399 confirmed AtMIR164a precursor was digested using the XbaI and Pst restriction enzymes, and
400 subsequently cloned into binary vector under the control of the CaMV 35S promoter. Once
401 cleaved, the mature *AtMIR164a* has the exact sequence of the mature *SlmiR164* (Accessions
402 for miRbase; http://www.mirbase.org/; AtMIR164: MI0000197; SlmiR164: MI0027570). The
403 genetic transformation was made in *Slglk2 Solanum lycopersicum* (cv Micro Tom) background
404 according to Pino et al. (2010). T2 plants were grown as above described and non-senescent
405 (NS), early senescing (ES) and late senescing (LS) leaves were collected. Leaves stages were set
406 according to the untransformed genotype yellowish phenotype.
407 For subcellular localization and BiFC assays, *Nicotiana tabacum* plants were cultivated for 4
408 weeks in 1-L pots as described above.
409 To evaluate the capability of *SlORE1S02, SlORE1S03* and SlORE1S06 to recover *Atore1* mutant
410 phenotype, this mutant was independently transformed with the three tomato gene coding

411 sequences under the control of the constitutive CaMV 35S promoter. *A. thaliana* plants were
412 grown and transformed according to Balazadeh *et al.* (2010). Plants from three independent
413 lines of T2 generation were used for dark-induced senescence assay. A pool of 10 detached
414 leaves from three-month-old plants for each genotype were kept in darkness for seven days.

415 *SlORE1S02*-knockdown lines (L1, L3 and L6) were generated by constitutively expressing an
416 intron-spliced hairpin RNA (RNAi) construct of 186 bp targeted to *SlORE1S02*
417 (Solyc02g088180). The fragment was cloned into pK7GWIWG2(I) (Karimi et al, 2002) and
418 introduced in wild type *Solanum lycopersicum* (cv Micro Tom) background, which harbours the
419 wild-type *SlGLK2* allele, following the protocol described in Pino et al. (2010). Gas exchange
420 and chlorophyll fluorescence parameters were measured in the fifth leaf of 70-day-old plants
421 (YPL) and in the sixth leaf of 120-day-old plants (MPL) between 10 and 12 h and were
422 subsequently harvested for biochemical analyses and transcriptional profiling. T1 plants were
423 grown as above described. Pericarp samples from fruits at MG, BR1 and BR6 stages were
424 harvested. For tocopherol content determination, leaf and pericarp samples were dried by
425 lyophilization before extraction. For yield evaluation, an independent set of plants without any
426 destructive sampling was cultivated and all ripe fruits were sampled and weighted until the
427 plants reach 160-day-old when destructive harvest took place. At harvest time, aerial part was
428 weighted and harvest index calculated according to HI = (total ripe fruit mass)*100/(aerial part
429 mass + total ripe fruit mass). Brix was measured in ripe fruits with a refractometer DR201-95
430 (Kruss).
431
432 *Phylogenetic analysis*
433 For the phylogenetic analysis, all NAC transcriptions factors of *S. lycopersicum* and *A. thaliana*
434 (Supplemental Table S1) were retrieved from the Plant Transcription Factors Database
435 (http://planttfdb.cbi.pku.edu.cn/). The retrieved protein sequences were aligned by Clustal in
436 MEGA 6.0 software (Tamura et al. 2013) using default parameters. The tree reconstruction

437 from the obtained alignment was performed using PHYML 3.0 algorithm (Guindon et al. 2010)
438 hosted at http://www.hiv.lanl.gov/content/sequence/PHYML/interface.html with the
439 following parameters: LG substitution model, four substitutions rate categories, tree
440 optimization by topology and branch length and, improvement by subtree pruning and
441 regrafting. From the dataset, the proportion of invariable sites, equilibrium of frequencies and
442 gamma shape parameter were estimated. Branches were supported by SH-like support.
443
444 *qPCR and miRNA analysis*
445 RNA extraction, complementary DNA (cDNA) synthesis, primer design and qPCR assays were
446 performed as described by Quadrana et al. (2013). Primer sequences used are detailed in
447 Supplemental Table S5. Stem loop pulse reverse transcriptase were performed as
448 described previously in Varkonyi-Gasic et al., (2007) and modified 5'RACE were
449 performed as described in Morea et al. (2016). qPCR reactions were carried out in a
450 QuantStudio 6 Flex Real-Time PCR system (Applied Biosystems) using 2X Power SYBR Green
451 Master Mix reagent (Life Technologies) in a 14 µL final volume. Absolute fluorescence data
452 were analysed using the LinRegPCR software package (Ruijter et al. 2009) in order to obtain
453 quantitation cycle (Cq) values and calculate PCR efficiency. Expression values were normalised
454 against the geometric mean of two reference genes, *TIP41* and *EXPRESSED*, according to
455 Quadrana et al. (2013). A permutation test lacking sample distribution assumptions (Pfaffl et
456 al. 2002) was applied to detect statistical differences ($P < 0.05$) in expression ratios using the
457 algorithms in the fgStatistics software package version 17/05/2012 (Di Rienzo 2009).
458
459 *Subcellular localization and BiFC assay*
460 The full-length open reading frames encoding *AtORE1* (AT5G39610), *AtGLK2* (AT5G44190),
461 SlGLKs and SlORE1s were amplified using specific primers listed in Supplemental Table S5 and
462 cloned into pCR™ 8/GW/TOPO TA Cloning vector (Invitrogen). For the subcellular localization

463 experiment, each recombination cassette was amplified using the universal M13 pair of
464 primers and then recombined into the binary vector pK7FWG2 (Karimi et al., 2002) using LR
465 clonase. For BiFC assay, each entry vector was recombined into the binary vector pDEST-
466 VYCE(R)GW or pDEST-VYNE(R)GW (Gehl et al., 2009), which carry the C-teminal and N-teminal
467 fragment of Venus YFP, respectively, using LR Clonase. All BiFC fusion proteins were tagged at
468 the C-terminus. The binary vectors were introduced in *Agrobacterium tumefaciens* strain
469 GV3101. For subcellular localization, cultures were resuspended in infiltration buffer (50 mM
470 MES pH 5.6, 2 mM sodium phosphate buffer pH 7, 0.5% glucose and 200 µM acetosyringone
471 (Sigma-Aldrich)) to a final OD_{600} of 0.5, incubated for 3 h in the dark at room temperature, and
472 infiltrated into leaves of 4-week-old *Nicotiana tabacum* plants. For BiFC experiments, leaves
473 were co-infiltrated with a mix of both cultures at 0.5 OD_{600}. To avoid SlGLKs degradation, 100
474 µM of the proteasome inhibitor MG132 (Sigma-Aldrich #C2211) was added to the solution
475 before infiltrating. After 48 or 72 h for localization and BiFC experiments, respectively, the
476 transformed tissues were observed in a confocal laser microscope (Zeiss LSM 780-NLO). DAPI
477 staining was performed by infiltrating 10 µg/mL of water dissolved DAPI (Life Technologies
478 #D1306) 20 min before the confocal microscope observation. GFP signal was captured over a
479 508-553 nm range after excitation at 488nm, while DAPI fluorescence was excited at 405 nm
480 and captured over a 415-501 nm range.
481 The controls VYNE-Cnx6 and VYCE-Cnx6 constructs were kindly provided by Prof. Jörg Kudla,
482 Institute of Plant Biology and Biotechnology, Münster, Germany. CNX6 is a protein that
483 belongs to the complex of molybdopterin synthase involved in MoCo biosynthesis. As reported
484 in Gehl et al. (2009), when VYNE-Cnx6 and VYCE-Cnx6 fusion proteins (approximately 40 KDa),
485 are transiently co-expressed in *N. benthamiana* leaves by agroinfiltration, they localize not
486 only in the cytoplasm but also in the nucleus. This is due to their small size that allows the
487 diffusion through the nuclear pores, which exclusion size is 60 KDa. Thus, Cnx6 auto-

dimerization was used as positive control, while VYNE-Cnx6/SlGLK2-VYCE and VYCE-Cnx6/SlORE1S02-VYNE interactions were used as negative controls.

Leaf gas exchange and fluorescence measurements

Gas exchange and chlorophyll fluorescence parameters were measured using a portable open gas-exchange system incorporating infra-red CO_2 and water vapor analysers (LI-6400XT system; LI-COR) equipped with an integrated modulated chlorophyll fluorometer (LI-6400-40; LI-COR). Reference CO_2 concentration was held at 400 µmol mol^{-1} and leaf temperature at 28˚C for all measurements. Air humidity inside the leaf chamber was equivalent to values measured inside the greenhouse (approximately 75%). Carbon assimilation rate (*A*), leaf stomatal conductance (g_s), transpiration (*E*) and fluorescence parameters were measured at 800 µmol PPFD m^{-2} s^{-1}. For the values of minimal (*Fo*) and maximal (*Fm*) fluorescence and leaf dark respiration, leaves were dark-adapted for 30 min before a saturating pulse of light. The parameters derived from chlorophyll fluorescence, including dark-adapted PSII maximum quantum efficiency (*Fv/Fm*), proportion of open PSII centers (photochemical quenching, *qP*), PSII operating efficiency (Φ_{PSII}), non-photochemical quenching (NPQ) and electron transport rate (ETR) were calculated according to Maxwell and Johnson (2000).

Chloroplast number

Chloroplasts in leaf mesophyll cells were counted following the methodology described in Pyke (2011). Briefly, leaf pieces were fixed in 3.5% (v/v) glutaraldehyde solution for 1 h, then calcium ions were chelated by transfering the leaf samples to 0.1 M NaEDTA solution and keeping them for 4 h at 60°C and then overnight at 4°C. The pieces were transferred to a microscope slide and macerated with a blunt scalpel for tissue desintegration, and visualised by light microscopy.

Transmission electron microscopy

Leaf segments were fixed at 4 °C in Karnovsky's solution [2.5% (v/v) glutaraldehyde, 2% (v/v) paraformaldehyde in 0.1 M sodium phosphate buffer pH 7.2] for 24 h. After washing in buffer, the samples were post-fixed in buffered 1% (w/v) osmium tetroxide, washed, dehydrated in a graded series of acetone, and embedded in Spurr resin. The resin was polymerized at 60ºC. Ultrathin sections were stained with saturated uranyl acetate (Watson, 1958) and lead citrate (Reynolds, 1963), and observed using a Zeiss EM 900 transmission electron microscope.

Total soluble proteins, starch and soluble sugars quantification

Total soluble proteins extraction and quantification were performed as described in Jones et al. (1989). Starch and soluble sugars extraction were performed as described in Lira et al. (2014). Soluble sugar quantification was performed according to Mainardi et al. (2006). Briefly, 1 mL of the extract was evaporated under vacuum in a SpeedVac system. The residue was resuspended with 1 mL of ultrapure water and filtered through 0.22 um membrane. Soluble sugars (i.e., glucose, fructose, sucrose) were analysed by high performance anion exchange chromatography with pulsed amperometric detection (HPAEC-PAD; Dionex, Sunnyvale, CA, USA), using a Carbopac PA1 (250 x 4 mm, 5 um particle size, Dionex) in an isocratic run with 18 mM NaOH as mobile phase. The content of each sugar was calculated with the standard curves made with pure glucose, fructose and sucrose (Sigma-Aldrich, Co).

Tocopherol and pigment quantification

Tocopherols were extracted from approximately 25 mg dry weight as described in Almeida et al. (2015). The samples were adjusted to 4 mL final volume. Aliquots of 3 mL were dried under N_2 and dissolved in 200 µL of mobile phase composed of hexane/*tert*-butyl methyl ether (90:10). Chromatography was carried out on a Hewlett–Packard series 1100 HPLC system coupled with a fluorescence detector (Agilent Technologies series 1200) on a normal-phase

column (LiChrosphere® 100 Diol Si; 250 mm x 4.0 mm, 5 µm; Agilent Technologies, Germany) at room temperature, with the mobile phase running isocratically at 1 mL min^{-1}. Eluted compounds were detected by excitation at 295 nm and fluorescence was quantified at 330 nm.

Chlorophyll extraction was carried out as described in Porra et al. (1989). One mL of dimethylformamide (DMF) was added to 100 mg or 300 mg of fresh weight for leaf or fruit samples, respectively. After sonication for five min and further centrifugation of 9000 *g* for 10 min, the supernatant was collected. The procedure was repeated until total removal of tissue green colour. Spectrophotometer measurements were performed at 664 and 647 nm.

Carotenoid extraction was modified from Sérino et al. (2009). Aliquots of 200 mg of fresh weight were sequentially extracted with a solution of saturated NaCl, dichloromethane and hexane:diethyl ether (1:1). After centrifugation, the supernatant was collected and the last step was repeated three more times. Samples were dried by vacuum and dissolved in 200 µL of acetonitrile. Chromatography was carried out on Agilent Technologies series 1100 HPLC system on a normal-phase column Phenomenex (Luna C18; 250 x 4.6 mm; 5 µm particle diameter) at room temperature with a flow rate of 1 mL min^{-1}. The mobile phase was a gradient of ethyl acetate (A) and acetonitrile:water 9:1 (B): 0-4 min with 20% A/80% B; 4-30 min with 65% A/35% B; 30-35 min with 65% A/35% B; 35-40 min with 20% A/80% B. Eluted compounds were detected between 340-700 nm and quantified at 450 nm.

Data analyses

Differences in parameters were analyzed in Infostat software version 17/06/2015 (Di Rienzo et al. 2011). When the data set showed homoscedasticity, Student´s *t*-test ($P < 0.05$) was performed to compare transgenic lines against the control genotype. In the absence of homoscedasticity, a non-parametric comparison was performed by applying the Mann-Whitney test ($P < 0.05$). All values represent the mean of at least three biological replicates. A

parameter was considered to be affected by *SlORE1S02* silencing if at least two out of the three transgenic lines differed significantly from the untransformed genotype.

Supplemental Data

Supplemental Figure S1. Phylogenetic representation of the NAC subfamily of *Solanum lycopersicum* and *Arabidopsis thaliana*.

Supplemental Figure S2. Alignment of SlORE1s, AtORE1 and AtORS1.

Supplemental Figure S3. Chlorophyll and senescence marker transcript levels after 48 hours of senescence-inducing treatments.

Supplementary Figure S4. Nuclear subcellular localization of SlGLKs and SlORE1s proteins.

Supplemental Figure S5. *SlORE1S02* knockdown effectiveness. *SlORE1S02* mRNA level in young plant leaves (YPL), mature plant leaves (MPL), mature green fruits (MG), breaker +1 fruits (BR1) and breaker +6 fruits (BR6) of untransformed and *SlORE1S02* knockdown plants.

Supplemental Figure S6. *SlORE1S02* knockdown effect over *SlORE1S03* and *SlORE1S06* transcript abundance.

Supplemental Figure S7. Chloroplast ultrastructure of MPL leaves of *SlORE1S02*-knockdown and MT control genotype.

Supplemental Figure S8. *SlORE1S02*-knockdown effects on fruit morphology and size.

Supplemental Figure S9. Effect of *SlORE1S02* knockdown on fruit development and metabolism.

Supplemental Table S1. NAC sequences accessions used for phylogenetic reconstruction.

Supplemental Table S2. Relative transcript values of genes addressed in leaves of *OEmiR164a* lines.

Supplemental Table S3. Carotenoid, tocopherol and chlorophyll content in SlORE1S02-knockdown lines.

Supplemental Table S4. Relative transcript values of genes addressed in leaves and along fruit ripening of *SlORE1S02*-knockdown lines.

Supplemental Table S5. Primers used in the experiments.

Supplemental Figure S1. Phylogenetic representation of the NAC subfamily of *Solanum lycopersicum* and *Arabidopsis thaliana*. Phylogenetic reconstruction obtained from the alignment of all NAC transcription factors of *A. thaliana* and *S. lycopersicum* obtained from the Plant Transcription Factor Database. Three putative orthologs (in blue) were chosen, namely SlORE1S02, SlORE1S03 and SlORE1S06 accordingly to the chromosome position. Marked with green or red circles are the functionally characterised proteins from *A. thaliana* or *S. lycopersicum,* respectively

Supplemental Figure S2. Alignment of SlORE1s, AtORE1 and AtORS1. The subdomains A-E of the NAC domain are underlined. Shading threshold = 100%

Supplemental Figure S3. Chlorophyll and senescence marker transcript levels after 48 hours of senescence-inducing treatments. Images of the leaves after 48 hours of senescence-inducing treatments. Heat map indicating the relative transcript ratio of *SlGLK1* (Solyc07g053630) and *SlSAG12* (Solyc02g076910) normalized against values from samples harvested 0h and 48h after ethylene treatment, respectively. Values represent the mean from at least three biological replicates. Black colour = not detected. Statistically significant differences compared with the corresponding controls ($P < 0.05$) are coloured accordingly to the scale. Chlorophyll content in leaf samples. Values represent the mean ± SE from at least three biological replicates. Statistically significant differences compared to not-treated control are marked with asterisks ($P < 0.05$).

Supplementary Figure S4. Nuclear subcellular localization of SlGLKs and SlORE1s proteins. GFP fusion proteins were transiently expressed in *Nicotiana tabacum* leaves by infiltration with *Agrobacterium tumefaciens.* GFP, DAPI nuclear marker, bright-field and merged signals are indicated above the panels. Bars, 20 µm.

Supplemental Figure S5. *SlORE1S02* knockdown effectiveness. *SlORE1S02* mRNA level in young plant leaves (YPL), mature plant leaves (MPL), mature green fruits (MG), breaker +1 fruits (BR1) and breaker +6 fruits (BR6) of untransformed and *SlORE1S02* knockdown plants. Value mean ± SE of at least three biological replicates normalised against the respective sample from MT control genotype. Asterisks denote statistically significant differences between MT control and the transgenic lines ($P < 0.05$).

Supplemental Figure S6. *SlORE1S02* knockdown effect over *SlORE1S03* and *SlORE1S06* transcript abundance. Top: *SlORE1S03* and *SlORE1S06* mRNA level in young plant leaves (YPL) and mature plant leaves (MPL) from control genotype (MT) and *SlORE1S02*-knockdown plants. Value mean ± SE of at least three biological replicates normalised against the respective sample from MT control genotype. Asterisks denote statistically significant differences between MT control and the transgenic lines ($P < 0.05$). Bottom: detail of the alignment of the

coding sequence of *SlORE*s, the blue boxes highlight the region of *SlORE1S02* targeted by the RNAi construct. Each coloured arrow pair indicates the primers used for qPCR analysis. Threshold for shading = 100%.

Supplemental Figure S7. Chloroplast ultrastructure of MPL leaves of *SlORE1S02*-knockdown and MT control genotype. PG, plastoglobulus; G, granum.

Supplemental Figure S8. *SlORE1S02*-knockdown effects on fruit morphology and size. Morphology, diameter and weight of breaker+6 fruits from MT and *SlORE1S02*-knockdown genotypes. Values represent the mean ± SE from at least forty four biological replicates. Asterisks denote statistically significant differences to the MT control genotype ($P < 0.05$). Bar = 0.7 cm.

Supplemental Figure S9. Effect of *SlORE1S02* knockdown on fruit development and metabolism. **A**, Number of days from anthesis to reach breaker stage. Value mean ± SE of at least ten biological replicates. Asterisk denote statistically significant differences compared to the corresponding sample from MT control ($P < 0.05$). **B**, Total soluble protein (TSP) of mature green fruits (MG), breaker +1 fruits (BR1) and breaker +6 fruits (BR6) from MT control genotype and *SlORE1S02*-knockdown plants. Value mean ± SE of at least three biological replicates. Asterisk denote statistically significant values compared to the corresponding sample from MT control ($P < 0.05$).

Supplemental Table S1. NAC sequences accessions used for phylogenetic reconstruction.

Supplemental Table S2. Relative transcript values of genes addressed in leaves of *OEmiR164a* lines.

Supplemental Table S3. Carotenoid, tocopherol and chlorophyll content in SlORE1S02-knockdown lines.

Supplemental Table S4. Relative transcript values of genes addressed in leaves and along fruit ripening of *SlORE1S02*-knockdown lines.

Supplemental Table S5. Primers used in the experiments.

Acknowledgments

The authors thank Prof. Dr. Javier Palatnik from IBR, CONICET, Argentina, for providing the p35S:AtMiR164a construct and Dr. Tania Misuzu Shiga from FCF, USP, Brazil, for the assistance in soluble sugar quantification.

Table 1. Photosynthetic parameters of *SlORE1S02-knockdown* lines.

Genotype		*CO_2 assimilation (A) (µmol CO_2/m² s)*	*Electron transport rate (ETR) (µmol/m² s)*	*Photochemical quenching (qP)*	*Non-photochemical quenching (NPQ)*
MT	YPL	4.31 ± 0.21	65.80 ± 3.16	0.28 ± 0.01	1.69 ± 0.21
	MPL	3.92 ± 0.15	35.93 ± 3.90	0.18 ± 0.02	2.18 ± 0.21
L1	YPL	4.63 ± 0.64	75.51 ± 7.47	0.30 ± 0.03	1.57 ± 0.12
	MPL	**5.93 ± 0.84**	**49.91 ± 4.38**	**0.24 ± 0.02**	2.13 ± 0.04
L3	YPL	**8.55 ± 0.95**	70.13 ± 6.71	0.31 ± 0.03	2.23 ± 0.34
	MPL	**5.28 ± 0.46**	41.63 ± 1.34	0.21 ± 0.01	2.28 ± 0.19
L6	YPL	3.97 ± 0.46	66.31 ± 4.47	0.31 ± 0.02	1.87 ± 0.15
	MPL	**5.57 ± 0.08**	38.68 ± 2.98	0.21 ± 0.01	1.76 ± 0.18

Values represent mean ± SD of at least three biological replicates. Statistically significant differences to MT control are in bold.

Figure Legends

Figure 1. Phylogenetic representation of the NAC transcription factor subfamily that includes AtORE1 and SlORE1s. Detail of the phylogenetic reconstruction obtained from the alignment of the protein sequence of all NAC transcription factors of *Arabidopsis thaliana* (green) and *Solanum lycopersicum* (red) obtained from the Plant Transcription Factor Database (Supplemental Table 1). Three putative AtORE1 orthologs (in bold), named SlORE1S02, SlORE1S03 and SlORE1S06 according to their chromosome position, were identified.

Figure 2. Transcript profile of *SlORE1s* in response to senescence-inducing treatments. Transcript profile of *SlORE1*s in leaves of 4-week-old *in vitro*-grown plants after senescence-inducing treatments. Values represent the mean ± SE from at least three biological replicates normalized against the zero hour sample. Each treatment relative transcript ratio is expressed as the ratio between treatment value and the corresponding untreated control (*). Statistically significant differences relative to the zero hour treatment are represented with closed symbols ($P < 0.05$).

Figure 3. Transcript profile of *SlORE1s* along fruit development and ripening. IG: immature green stage; MG: mature green stage; BR: breaker stage; BRX: X days after breaker stage. Values represent the mean ± SE from at least three biological replicates normalized to the corresponding IG3 sample. Statistically significant differences are represented with letters ($P < 0.05$).

Figure 4. Regulation of *SlORE1*s by *SlmiR164*. **A**, Highlight of the alignment of *SlORE1*s and *SlmiR164* showing the putative binding site. The validation by a modified 5' RACE assay identified cleaved transcripts of *SlORE1S03* and *SlORE1S06.* The red arrowhead and numbers on the right indicate the inferred cleavage site and the fraction of positive cloned PCR products ending at the site, respectively. Shading threshold of alignment = 75%. **B**, Heatmap representing the transcript profile of non-senescent (NS), early senescing (ES) and late senescing (LS) leaves of wild type control (WT) and *OEmiR164a* (lines miR_2 and miR_3) genotype. Values represent mean of at least three biological replicates normalysed against the NS WT sample. Statistically significant differences in comparison to NS WT are represented as coloured squares ($P < 0.05$). The relative transcript values are detailed in Supplemental Table S2. **C**, Chlorophyll content in NS, ES and LS leaves. Values represent the mean ± SE from at least three biological replicates. Asterisks denote statistically significant differences to WT control ($P < 0.05$.)

Figure 5. Analysis of SlGLKs and SlORE1s protein-protein interaction by Bimolecular Fluorescent Complementation (BiFC). VYNE and VYCE fusion proteins were transiently expressed in *N. tabacum* leaves by infiltration with *A. tumefaciens.* VYNE-Cnx6/VYCE-Cnx6 and AtORE1/AtGLK2 (Gehl et al., 2009) were used as technical and biological positive controls, respectively. VYNE-Cnx6/SlGLK2-VYCE and VYCE-Cnx6/SlORE1S02-VYNE interactions were used as negative controls. SlOREs/SlGLKs interaction was confirmed as evidenced by the YFP fluorescence detected. YFP, DAPI nuclear marker, bright-field and merged signals are indicated above the panels. Bars = 20 µm, except in VYNE-Cnx6/VYCE-Cnx6 images = 40 µm.

Figure 6. *SlORE1s* partially recover *Atore1* senescence impairment. Detached leaves from three-month-old Col-0, *Atore1* mutant*, Atore1-OE:SlORE1S02, Atore1-OE:SlORE1S03* and *Atore1-OE:SlORE1S06* plants were kept in darkness for seven days to induce senescence. While *Atore1* displayed no signs of senescence, the yellowish colour of the genotypes overexpressing *SlORE1s* hints an ongoing senescence program, yet not to the extent observed in the Col-0 genotype. Bar = 1 cm.

738
739 **Figure 7.** *SlORE1S02-knockdown* affects leaf aging. **A**, Chlorophyll content in leaves. Values
740 represent the mean ± SE from at least three biological replicates. Asterisks denote statistically
741 significant differences to MT control ($P < 0.05$). YPL: young plant leaves; MPL: mature plant
742 leaves. **B**, Number of chloroplasts per mesophyll cell of MPL. Values represent the mean ± SE
743 from at least 45 cells. Asterisks denote statistically significant differences to MT control ($P <$
744 0.05). **C**, *SlGLK1* and *SlSAG12* transcript ratio in YPL and MPL leaves. Values represent the mean
745 ± SE from at least three biological replicates normalised against the respective sample from MT
746 control. Asterisks denote statistically significant differences to MT control ($P < 0.05$). The
747 relative transcript values are available in Supplemental Table S4. **D,** *SlORE1S02*-knockdown
748 effect on dark-induced senescence in tomato leaves. Detached leaflets from 120-day-old
749 plants kept ten days in darkness retain greenness, while MT control leaflets turned yellow. Bar
750 = 5 cm.
751
752 **Figure 8.** *SlORE1S02*-knockdown increases yield and *brix*. **A**, Harvest index, aerial part weight
753 and ripe fruit number in MT and *SlORE1S02*-knockdown lines. Values represent the mean ± SE
754 from at least six biological replicates. Asterisks denote statistically significant differences
755 compared to MT control genotype ($P < 0.05$). **B**, Total soluble solids of ripe fruits measured in
756 *brix* units. Values represent the mean ± SE from at least twelve biological replicates. Asterisks
757 denote statistically significant differences compared to MT control genotype ($P < 0.05$).
758
759 **Figure 9.** *SlORE1S02*-knockdown alters sugar profile in leaves and fruits. Content of starch and
760 soluble sugars in leaves and fruits of *SlORE1S02*-knockdown lines. Values represent the mean ±
761 SE from at least three biological replicates. Asterisks denote statistically significant differences
762 to MT control genotype ($P < 0.05$). ND: Not detected. YPL, young plant leaves; MPL, mature
763 plant leaves; MG, mature green stage; BR, breaker; BR6: 6 days after BR, respectively.
764
765 **Figure 10.** Isoprenoid metabolism. Schematic representation of the interconnection between
766 chlorophyll synthesis and degradation (green), carotenogenesis (orange) and tocopherol
767 biosynthetic (blue) pathways. Dotted lines denote that intermediate steps were omitted. The
768 heatmap represents statistically significant differences in relative transcript and metabolite
769 amounts detected in *SlORE1S02*-knockdown lines compared to the corresponding organ of MT
770 control genotype ($P < 0.05$). For simplicity, the mean of the three transgenic line values is
771 represented when, at least, two were statistically significant different than MT control. The
772 absolute metabolite and relative transcript values are detailed in Supplemental Table S3 and
773 S4. Black and grey colours indicate that transcripts were not detected or not addressed,
774 respectively. Enzymes and compounds are named according to the following abbreviations:
775 GGDR, geranylgeranyl diphosphate reductase; PSY, phytoene synthase; PDS, phytoene
776 desaturase; LCYβ, chloroplast-specific β-lycopene cyclase; CYCβ, chromoplast-specific β-
777 lycopene cyclase; GGDP, geranylgeranyl diphosphate; PDP, phytyl diphosphate; PP, phytyl
778 phosphate; CHLG, chlorophyll synthase; PPH, pheophytinase; PPHL1, pheophytinase-like 1;
779 pFCC, primary fluorescent chlorophyll catabolite; VTE5, phytol kinase; VTE6, phytyl phosphate
780 kinase; MPBQ, 2-methyl-6-geranylgeranylbenzoquinol; VTE1, tocopherol cyclase; VTE2,
781 homogentisate phytyl transferase; VTE3, 2,3-dimethyl-5-phytylquinol methyltransferase; VTE4,
782 tocopherol C-methyl transferase; MEP, methylerythritol 4-phosphate. Adapted from Almeida
783 et al. (2016).
784
785

Parsed Citations

Almeida J, Asís R, Molineri VN, Sestari I, Lira BS, Carrari F, Peres LEP, Rossi M (2015) Fruits from ripening impaired, chlorophyll degraded and jasmonate insensitive tomato mutants have altered tocopherol content and composition. Phytochemistry 111: 72-83.
Pubmed: Author and Title
CrossRef: Author and Title
Google Scholar: Author Only Title Only Author and Title

Almeida J, Azevedo MDS, Spicher L, Glauser G, vom Dorp K, Guyer L, Carranza AV, Asis R, Souza AP, et al (2016) Down-regulation of tomato PHYTOL KINASE strongly impairs tocopherol biosynthesis and affects prenyllipid metabolism in an organ-specific manner. Journal of Experimental Botany, 67: 919-934.
Pubmed: Author and Title
CrossRef: Author and Title
Google Scholar: Author Only Title Only Author and Title

Balazadeh S, Riano-Pachon DM, Mueller-Roeber B (2008) Transcription factors regulating leaf senescence in Arabidopsis thaliana. Plant Biology 10: 63-75.
Pubmed: Author and Title
CrossRef: Author and Title
Google Scholar: Author Only Title Only Author and Title

Balazadeh S, Siddiqui H, Allu AD, Matallana-Ramirez LP, Caldana C, Mehrnia M, Zanor M, Köhler B, Mueller-Roeber B (2010) A gene regulatory network controlled by the NAC transcription factor ANAC092/AtNAC2/ORE1 during salt-promoted senescence. The Plant Journal 62(2): 250-264.
Pubmed: Author and Title
CrossRef: Author and Title
Google Scholar: Author Only Title Only Author and Title

Barker L, Kühn C, Weise A, Schulz A, Gebhardt C, Hirner B, Hellmann H, Schulze W, Ward JM, Frommer WB (2000) SUT2, a putative sucrose sensor in sieve elements. The Plant Cell 12(7): 1153-1164.
Pubmed: Author and Title
CrossRef: Author and Title
Google Scholar: Author Only Title Only Author and Title

Chrost B, Falk J, Kernebeck B, Mölleken H, Krupinska K (1999) Tocopherol Biosynthesis in Senescing Chloroplasts-A Mechanism to Protect Envelope Membranes against Oxidative Stress and a Prerequisite for Lipid Remobilization?. In The Chloroplast: From Molecular Biology To Biotechnology: 171-176. Springer.
Pubmed: Author and Title
CrossRef: Author and Title
Google Scholar: Author Only Title Only Author and Title

Di Rienzo JA (2009) Statistical software for the analysis of experiments of functional genomics. RDNDA, Argentina: http://sites. google. com/site/fgStatistics.
Pubmed: Author and Title
CrossRef: Author and Title
Google Scholar: Author Only Title Only Author and Title

Di Rienzo JA, Casanoves F, Balzarini MG, Gonzalez L, Tablada M, Robledo YC (2011) InfoStat versión 2011. Grupo InfoStat, FCA, Universidad Nacional de Córdoba, Argentina. http://www.infostat.com.ar, 8: 195-199.
Pubmed: Author and Title
CrossRef: Author and Title
Google Scholar: Author Only Title Only Author and Title

Fitter DW, Martin DJ, Copley MJ, Scotland RW, Langdale JA (2002) GLK gene pairs regulate chloroplast development in diverse plant species. The Plant Journal 31: 713-727.
Pubmed: Author and Title
CrossRef: Author and Title
Google Scholar: Author Only Title Only Author and Title

Garapati P, Xue GP, Munné-Bosch S, Balazadeh S (2015) Transcription factor ATAF1 in Arabidopsis promotes senescence by direct regulation of key chloroplast maintenance and senescence transcriptional cascades. Plant Physiolog 168: 1122-1139
Pubmed: Author and Title
CrossRef: Author and Title
Google Scholar: Author Only Title Only Author and Title

Gehl C, Waadt R, Kudla J, Mendel RR, Hänsch R (2009) New GATEWAY vectors for high throughput analyses of protein-protein interactions by bimolecular fluorescence complementation. Molecular Plant, 2: 1051-1058.
Pubmed: Author and Title
CrossRef: Author and Title
Google Scholar: Author Only Title Only Author and Title

Gregersen PL, Culetic A, Boschian L, Krupinska K (2013) Plant senescence and crop productivity. Plant Molecular Biology, 82: 603-622.
Pubmed: Author and Title
CrossRef: Author and Title
Google Scholar: Author Only Title Only Author and Title

Guindon S, Dufayard JF, Lefort V, Anisimova M, Hordijk W, Gascuel O (2010) New algorithms and methods to estimate maximum-likelihood phylogenies: assessing the performance of PhyML 3.0. Systematic Biology, 59: 307-321.

Pubmed: Author and Title
CrossRef: Author and Title
Google Scholar: Author Only Title Only Author and Title

Havaux M, Eymery F, Porfirova S, Rey P, Dörmann P (2005) Vitamin E protects against photoinhibition and photooxidative stress in Arabidopsis thaliana. The Plant Cell, 17: 3451-3469.
Pubmed: Author and Title
CrossRef: Author and Title
Google Scholar: Author Only Title Only Author and Title

He XJ, Mu RL, Cao WH, Zhang ZG, Zhang JS, Chen SY (2005) AtNAC2, a transcription factor downstream of ethylene and auxin signaling pathways, is involved in salt stress response and lateral root development. The Plant Journal, 44: 903-916.
Pubmed: Author and Title
CrossRef: Author and Title
Google Scholar: Author Only Title Only Author and Title

Jones CG, Daniel-Hare J, Compton SJ (1989) Measuring plant protein with the Bradford assay. Journal of Chemical Ecology, 15: 979-992.
Pubmed: Author and Title
CrossRef: Author and Title
Google Scholar: Author Only Title Only Author and Title

Karimi M, Inzé D, Depicker A (2002) GATEWAY™ vectors for Agrobacterium-mediated plant transformation. Trends In Plant Science, 7: 193-195.
Pubmed: Author and Title
CrossRef: Author and Title
Google Scholar: Author Only Title Only Author and Title

Kim JH, Chung KM, Woo HR (2011) Three positive regulators of leaf senescence in Arabidopsis, ORE1, ORE3 and ORE9, play roles in crosstalk among multiple hormone-mediated senescence pathways. Genes & Genomics, 33: 373-381.
Pubmed: Author and Title
CrossRef: Author and Title
Google Scholar: Author Only Title Only Author and Title

Kim JH, Woo HR, Kim J, Lim PO, Lee IC, Choi SH, Hwang D, Nam HG (2009) Trifurcate feed-forward regulation of age-dependent cell death involving miR164 in Arabidopsis. Science, 323: 1053-1057.
Pubmed: Author and Title
CrossRef: Author and Title
Google Scholar: Author Only Title Only Author and Title

Liang C, Wang Y, Zhu Y, Tang J, Hu B, Liu L, Ou S, Wu H, Sun X, Chu C (2014) OsNAP connects abscisic acid and leaf senescence by fine-tuning abscisic acid biosynthesis and directly targeting senescence-associated genes in rice. Proceedings of the National Academy of Sciences, 111: 10013-10018.
Pubmed: Author and Title
CrossRef: Author and Title
Google Scholar: Author Only Title Only Author and Title

Lin YP, Wu MC, Charng YY (2016) Identification of a chlorophyll dephytylase involved in chlorophyll turnover in Arabidopsis. The Plant Cell, 28: 2974-2990.
Pubmed: Author and Title
CrossRef: Author and Title
Google Scholar: Author Only Title Only Author and Title

Lira BS, de Setta N, Rosado D, Almeida J, Freschi L, Rossi M (2014) Plant degreening: evolution and expression of tomato (Solanum lycopersicum) dephytylation enzymes. Gene, 546: 359-366.
Pubmed: Author and Title
CrossRef: Author and Title
Google Scholar: Author Only Title Only Author and Title

Lira BS, Rosado D, Almeida J, de Souza AP, Buckeridge MS, Purgatto E, Guyer L, Hörtensteiner S, Freschi L, Rossi M (2016) Pheophytinase knockdown impacts carbon metabolism and nutraceutical content under normal growth conditions in tomato. Plant and Cell Physiology, 57: 642-653.
Pubmed: Author and Title
CrossRef: Author and Title
Google Scholar: Author Only Title Only Author and Title

Liu L, Zhou Y, Szczerba MW, Li X, Lin Y (2010) Identification and application of a rice senescence-associated promoter. Plant Physiology, 153:1239-1249.
Pubmed: Author and Title
CrossRef: Author and Title
Google Scholar: Author Only Title Only Author and Title

Liu L, Shao Z, Zhang M, Wang Q (2015) Regulation of carotenoid metabolism in tomato. Molecular Plant, 8:28-39.
Pubmed: Author and Title
CrossRef: Author and Title
Google Scholar: Author Only Title Only Author and Title

Mainardi JA, Purgatto E, Vieira-Junior A, Bastos WA, Cordenunsi BR, Nascimento JRO, Lajolo FM (2006). The effects of ethylene and 1-MCP on gene expression and activity profile of starch phosphorylase during banana ripening. Journal of Agricultural and Food Chemistry, 54: 7294-7299.

Pubmed: Author and Title
CrossRef: Author and Title
Google Scholar: Author Only Title Only Author and Title

Maxwell K, Johnson GN (2000) Chlorophyll fluorescence—a practical guide. Journal Of Experimental Botany 51: 659-668.
Pubmed: Author and Title
CrossRef: Author and Title
Google Scholar: Author Only Title Only Author and Title

Mitsuda N, Seki M, Shinozaki K, Ohme-Takagi M (2005) The NAC transcription factors NST1 and NST2 of Arabidopsis regulate secondary wall thickenings and are required for anther dehiscence. The Plant Cell, 17:2993-3006.
Pubmed: Author and Title
CrossRef: Author and Title
Google Scholar: Author Only Title Only Author and Title

Morea EGO, da Silva EM, e Silva GFF, Valente GT, Rojas CHB, Vincentz M, Nogueira FTS (2016) Functional and evolutionary analyses of the miR156 and miR529 families in land plants. BMC Plant Biology, 16:40.
Pubmed: Author and Title
CrossRef: Author and Title
Google Scholar: Author Only Title Only Author and Title

Nguyen CV, Vrebalov JT, Gapper NE, Zheng Y, Zhong S, Fei Z, Giovannoni JJ (2014) Tomato GOLDEN2-LIKE transcription factors reveal molecular gradients that function during fruit development and ripening. The Plant Cell, 26:585-601.
Pubmed: Author and Title
CrossRef: Author and Title
Google Scholar: Author Only Title Only Author and Title

Oh SA, Park JH, Lee GI, Paek KH, Park SK, Nam HG (1997) Identification of three genetic loci controlling leaf senescence in Arabidopsis thaliana. The Plant Journal, 12:527-535.
Pubmed: Author and Title
CrossRef: Author and Title
Google Scholar: Author Only Title Only Author and Title

Olsen AN, Ernst HA, Leggio LL, Skriver K (2005) NAC transcription factors: structurally distinct, functionally diverse. Trends in Plant Science, 10:79-87.
Pubmed: Author and Title
CrossRef: Author and Title
Google Scholar: Author Only Title Only Author and Title

Pfaffl MW, Horgan GW, Dempfle L (2002) Relative expression software tool (REST©) for group-wise comparison and statistical analysis of relative expression results in real-time PCR. Nucleic Acids Research, 30:e36-e36.
Pubmed: Author and Title
CrossRef: Author and Title
Google Scholar: Author Only Title Only Author and Title

Pino LE, Lombardi-Crestana S, Azevedo MS, Scotton DC, Borgo L, Quecini V, Figueira A, Peres LE (2010) The Rg1 allele as a valuable tool for genetic transformation of the tomato'Micro-Tom'model system. Plant Methods, 6:23.
Pubmed: Author and Title
CrossRef: Author and Title
Google Scholar: Author Only Title Only Author and Title

Porra RJ, Thompson WA, Kriedemann PE (1989) Determination of accurate extinction coefficients and simultaneous equations for assaying chlorophylls a and b extracted with four different solvents: verification of the concentration of chlorophyll standards by atomic absorption spectroscopy. Biochimica et Biophysica Acta (BBA)-Bioenergetics, 975:384-394.
Pubmed: Author and Title
CrossRef: Author and Title
Google Scholar: Author Only Title Only Author and Title

Powell AL, Nguyen CV, Hill T, Cheng KL, Figueroa-Balderas R, Aktas H, Ashrafi H, Pons C, Fernández-Muñoz R, et al. (2012) Uniform ripening encodes a Golden 2-like transcription factor regulating tomato fruit chloroplast development. Science, 336:1711-1715.
Pubmed: Author and Title
CrossRef: Author and Title
Google Scholar: Author Only Title Only Author and Title

Puranik S, Sahu PP, Srivastava PS, Prasad M (2012) NAC proteins: regulation and role in stress tolerance. TRENDS IN PLANT SCIENCE, 17:369-381.
Pubmed: Author and Title
CrossRef: Author and Title
Google Scholar: Author Only Title Only Author and Title

Pyke K (2011) Analysis of plastid number, size, and distribution in Arabidopsis plants by light and fluorescence microscopy. In Chloroplast Research in Arabidopsis: Methods and Protocols, Volume I: 19-32.
Pubmed: Author and Title
CrossRef: Author and Title
Google Scholar: Author Only Title Only Author and Title

Quadrana L, Almeida J, Otaiza SN, Duffy T, Da Silva JVC, de Godoy F, Asís R, Bermúdez L, Fernie A, Carrari F, et al. (2013) Transcriptional regulation of tocopherol biosynthesis in tomato. Plant Molecular Biology, 81: 309-325.
Pubmed: Author and Title
CrossRef: Author and Title

Google Scholar: Author Only Title Only Author and Title

Rauf M, Arif M, Dortay H, Matallana-Ramírez LP, Waters MT, Nam HG, Lim P, Mueller-Roeber B, Balazadeh S (2013) ORE1 balances leaf senescence against maintenance by antagonizing G2-like-mediated transcription. EMBO Reports, 14:382-388.
Pubmed: Author and Title
CrossRef: Author and Title
Google Scholar: Author Only Title Only Author and Title

Reynolds ES (1963). The use of lead citrate at high pH as an electron-opaque stain in electron microscopy. The Journal of Cell Biology, 17:208.
Pubmed: Author and Title
CrossRef: Author and Title
Google Scholar: Author Only Title Only Author and Title

Rossi M, Bermudez L, Carrari F (2015) Crop yield: challenges from a metabolic perspective. Current Opinion in Plant Biology, 25:79-89.
Pubmed: Author and Title
CrossRef: Author and Title
Google Scholar: Author Only Title Only Author and Title

Ruijter JM, van der Velden S, Ilgun A (2009) LinReg PCR (11.0). Analysis of quantitative.
Pubmed: Author and Title
CrossRef: Author and Title
Google Scholar: Author Only Title Only Author and Title

Sakuraba Y, Jeong J, Kang MY, Kim J, Paek NC, Choi G (2014) Phytochrome-interacting transcription factors PIF4 and PIF5 induce leaf senescence in Arabidopsis. Nature Communications, 5:4636.
Pubmed: Author and Title
CrossRef: Author and Title
Google Scholar: Author Only Title Only Author and Title

Se´rino S, Gomez L, Costagliola GUY, Gautier H (2009) HPLC assay of tomato carotenoids: validation of a rapid microextraction technique. Journal of Agricultural And Food Chemistry, 57:8753-8760.
Pubmed: Author and Title
CrossRef: Author and Title
Google Scholar: Author Only Title Only Author and Title

Shalygo N, Czarnecki O, Peter E, Grimm B (2009) Expression of chlorophyll synthase is also involved in feedback-control of chlorophyll biosynthesis. Plant Molecular Biology, 71:425-436.
Pubmed: Author and Title
CrossRef: Author and Title
Google Scholar: Author Only Title Only Author and Title

Song Y, Yang C, Gao S, Zhang W, Li L, Kuai B (2014) Age-triggered and dark-induced leaf senescence require the bHLH transcription factors PIF3, 4, and 5. Molecular plant, 7:1776-1787.
Pubmed: Author and Title
CrossRef: Author and Title
Google Scholar: Author Only Title Only Author and Title

Stepinski D (2012) Immunofluorescent localization of ubiquitin and proteasomes in nucleolar vacuoles of soybean root meristematic cells. European Journal of Histochemistry, 56: 13.
Pubmed: Author and Title
CrossRef: Author and Title
Google Scholar: Author Only Title Only Author and Title

Stepinski D (2014) Functional ultrastructure of the plant nucleolus. Protoplasma, 251:1285-1306.
Pubmed: Author and Title
CrossRef: Author and Title
Google Scholar: Author Only Title Only Author and Title

Suguiyama VF, da Silva EA, Meirelles ST, Centeno DDC, Braga MR (2014) Leaf metabolite profile of the Brazilian resurrection plant Barbacenia purpurea Hook.(Velloziaceae) shows two time-dependent responses during desiccation and recovering. Frontiers in Plant Science, 5:96.
Pubmed: Author and Title
CrossRef: Author and Title
Google Scholar: Author Only Title Only Author and Title

Swartzberg D, Dai N, Gan S, Amasino R, Granot D (2006) Effects of cytokinin production under two SAG promoters on senescence and development of tomato plants. Plant Biology, 8:579-586.
Pubmed: Author and Title
CrossRef: Author and Title
Google Scholar: Author Only Title Only Author and Title

Sýkorová B, Kurešová G, Daskalova S, Trcková M, Hoyerová K, Raimanová I, Motyka V, Trávnícková A, Elliott MC, Kamínek M (2008) Senescence-induced ectopic expression of the A. tumefaciens ipt gene in wheat delays leaf senescence, increases cytokinin content, nitrate influx, and nitrate reductase activity, but does not affect grain yield. Journal of Experimental Botany, 59:377-387.
Pubmed: Author and Title
CrossRef: Author and Title
Google Scholar: Author Only Title Only Author and Title

Tamura K, Stecher G, Peterson D, Filipski A, Kumar S (2013) MEGA6: molecular evolutionary genetics analysis version 6.0. Molecular Biology and Evolution, 30:2725-2729.
Pubmed: Author and Title
CrossRef: Author and Title
Google Scholar: Author Only Title Only Author and Title

Tang X, Miao M, Niu X, Zhang D, Cao X, Wang A, Giovannoni JJ, Liu Y (2015) UV-damaged DNA binding protein-1 and de-etiolated-1 regulate golden 2-like transcription factor by assembling a cullin 4-based ubiquitin ligase in tomato. New Phytologist, 209:1028-1039.
Pubmed: Author and Title
CrossRef: Author and Title
Google Scholar: Author Only Title Only Author and Title

Thomas H (2013) Senescence, ageing and death of the whole plant. New Phytologist, 197:696-711.
Pubmed: Author and Title
CrossRef: Author and Title
Google Scholar: Author Only Title Only Author and Title

Thomas H, Ougham H (2014) The stay-green trait. Journal of Experimental Botany, 65:3889-3900.
Pubmed: Author and Title
CrossRef: Author and Title
Google Scholar: Author Only Title Only Author and Title

Un YJ, Cao ML, Xu CG, Chen H, Wei J, Zhang QF (2002) Cultivating Rice with Delaying Leaf-Senescence by Ysagîi-IPT Gene Transformation. Acta Botanica Sinica, 44:1333-1338.
Pubmed: Author and Title
CrossRef: Author and Title
Google Scholar: Author Only Title Only Author and Title

Varkonyi-Gasic E, Wu R, Wood M, Walton EF, Hellens RP (2007) Protocol: a highly sensitive RT-PCR method for detection and quantification of microRNAs. Plant Methods, 3 :12.
Pubmed: Author and Title
CrossRef: Author and Title
Google Scholar: Author Only Title Only Author and Title

Waters BM, Uauy C, Dubcovsky J, Grusak MA (2009) Wheat (Triticum aestivum) NAM proteins regulate the translocation of iron, zinc, and nitrogen compounds from vegetative tissues to grain. Journal of Experimental Botany, 60:4263-4274.
Pubmed: Author and Title
CrossRef: Author and Title
Google Scholar: Author Only Title Only Author and Title

Waters MT, Moylan EC, Langdale JA (2008) GLK transcription factors regulate chloroplast development in a cell-autonomous manner. The Plant Journal, 56:432-444.
Pubmed: Author and Title
CrossRef: Author and Title
Google Scholar: Author Only Title Only Author and Title

Waters MT, Wang P, Korkaric M, Capper RG, Saunders NJ, Langdale JA (2009) GLK transcription factors coordinate expression of the photosynthetic apparatus in Arabidopsis. The Plant Cell, 21:1109-1128.
Pubmed: Author and Title
CrossRef: Author and Title
Google Scholar: Author Only Title Only Author and Title

Watson ML (1958) Staining of tissue sections for electron microscopy with heavy metals II. Application of solutions containing lead and barium. The Journal of Biophysical and Biochemical Cytology, 4:727-730.
Pubmed: Author and Title
CrossRef: Author and Title
Google Scholar: Author Only Title Only Author and Title

Wu XY, Kuai BK, Jia JZ, Jing HC (2012) Regulation of leaf senescence and crop genetic improvement. Journal of Integrative Plant Biology, 54:936-952.
Pubmed: Author and Title
CrossRef: Author and Title
Google Scholar: Author Only Title Only Author and Title

Zhang MP, Zhang CJ, Yu GH, Jiang YZ, Strasser RJ, Yuan ZY, Yang X, Chen G (2010) Changes in chloroplast ultrastructure, fatty acid components of thylakoid membrane and chlorophyll a fluorescence transient in flag leaves of a super-high-yield hybrid rice and its parents during the reproductive stage. Journal of Plant Physiology, 167:277-285.
Pubmed: Author and Title
CrossRef: Author and Title
Google Scholar: Author Only Title Only Author and Title